Accelerating Nonequilibrium Green functions simulations: the G1-G2 scheme and beyond

Michael Bonitz, Jan-Philip Joost, Karsten Balzer, Hannes Ohldag,
Christopher Makait, and Erik Schroedter
Institut für Theoretische Physik und Astrophysik, CAU Kiel

in collaboration with
Iva Brezinova, Anna Niggas und Richard Wilhelm (TU Vienna)

PNGF 8 conference
Örebro, August 2023

Progress in Nonequilibrium Green functions (since 1999)

Christian-Albrechts-Universität zu Kiel
Mathematisch-Naturwissenschaftliche Fakultät

PNGF2: August 2002 in flooded Dresden

from left (selection): Irena Knezevic, Manfred Schlanges, David Ferry, Norman Horing, Frank Jahnke, Carlo Jacoboni, John Barker, Alex Abrikosov (Nobel prize 2003, † 2017), Leonid Keldysh († 2016), Robert, Roland Zimmermann, Jörn Knoll, Pavel, Antti Jauho, Rolf Binder, Paul Martin († 2016)

veterans at PNGF8

Outline

1. Motivation: Finite 2D quantum materials
2. Lattice models: Hubbard, PPP
3. Equilibrium GF: LDOS of quantum materials. Löwdin's "symmetry dilemma"
4. NEGF. Keldysh-Kadanoff–Baym equations. Selfenergies
5. Accelerating NEGF
   - 1: Hartree-Fock-GKBA
   - 2: G1–G2 scheme. Advanced selfenergies
   - Scalings and problems of the G1–G2 scheme
6. Nonequilibrium dynamics of 2D quantum materials
   - dynamics following laser excitation
   - charge transfer and ultrafast electron emission due to ion impact
7. Extended time-linear NEGF embedding schemes

Finite 2D quantum materials

Graphene Nanostructures: additional confinement of electrons

Graphene:

- lots of interesting electronic and transport properties
- however, **no bandgap**
- therefore, not suitable for application in electronics, e.g. transistors
- solution: quantum confinement in finite graphene nanostructures e.g. clusters, flakes or **nanoribbons**

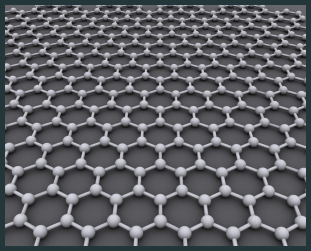

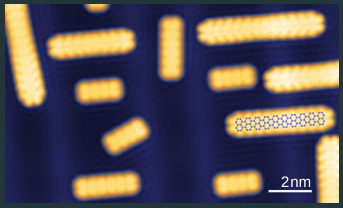

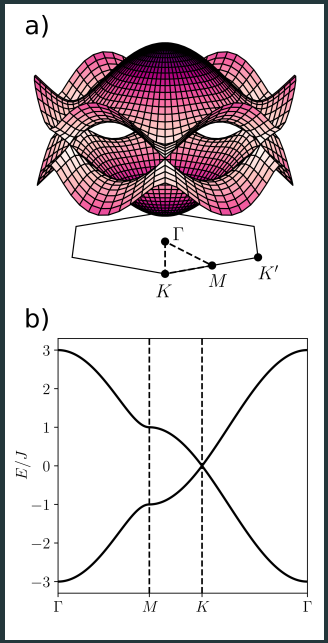

Potential Applications of Graphene: towards petahertz electronics[1]

Experiments by P. Hommelhoff *et al.*: logic gate for lightwave electronics, variation of carrier envelope phase ϕ_{CE} of few cycle fs-laser pulse

a: momentum asymmetry ($A(t)$) creates $f_c(-k) \neq f_c(k)$ and net current

b: real space asymmetry ($E(t)$) of density creates net polarization

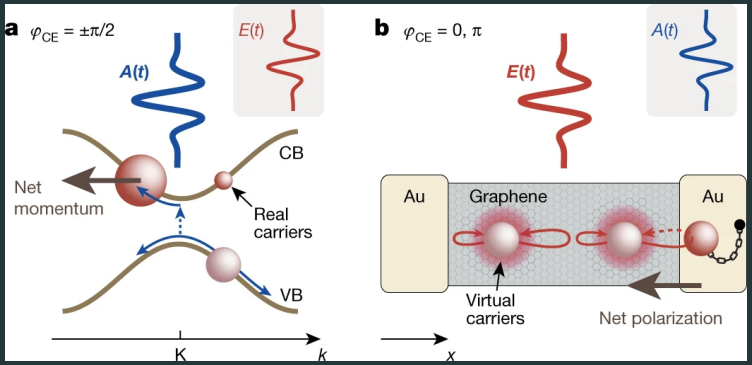

[1] Boolakee et al., Nature **605**, 251 (2022)

Potential of Graphene and TMDCs: Strong electronic correlations[4]

- twisted bilayer graphene: Moiré lattices predicted, realization of strong correlation phenomena (low density, $r_s = \bar{r}/a_B \gtrsim 35$), including electron liquid, Wigner crystal, cf. Ref. 4
- even more flexibility: TMDC monoloyers, twisted bilayers[2]
- STM experiments on WSe_2/WS_2 bilayers[3] confirm electron localization. Even crystal-like behavior ("generalized Wigner crystal") reported for certain fillings n:

b: $n = 1$, c: $n = 2/3$, d: $n = 1/3$, e: $n = 1/2$

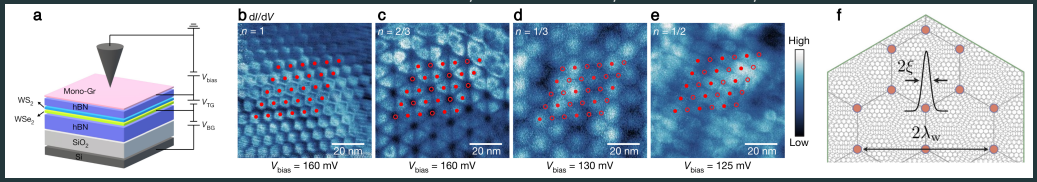

[2] A. MacDonald *et al.*, Phys. Rev. Lett. **121**, 026402 (2018)
[3] H. Li *et al.*, Nature **597** 650 (2021)
[4] M. Bonitz and J.-P. Joost, *View point*, Physik Journal **20** (12), 20-21 (2021)

Challenges in Condensed Matter Physics and Quantum Chemistry

- finite size systems (molecules) of ~ 10–1000 atoms
- example: polycyclic aromatic hydrocarbon (PAH)
- going beyond a mean-field treatment of the electronic interactions is challenging
- exact solution (CI, MCSCF, etc.) not possible because configuration space grows exponentially

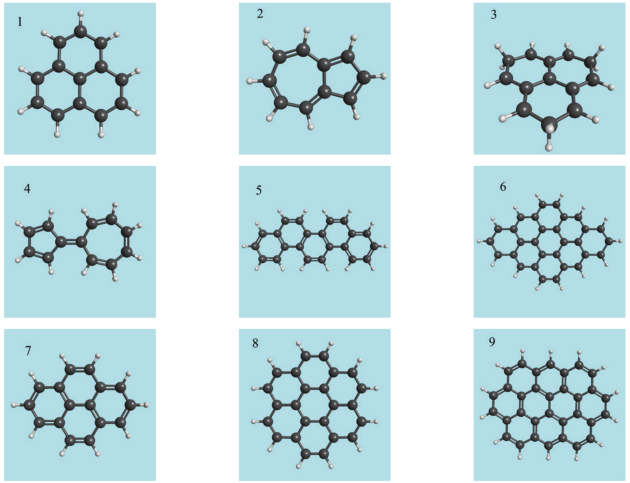

Figure 1. PAH referred to in this work: (1) phenalenide anion (13 π orbitals and 14 valence electrons), (2) azulene, (3) 2, 5, 8 trihydro-phenalenyl, (4) pentaheptafulvalene, (5) picene, (6) dibenzo[bc,kl]coronene (7) pyrene, (8) coronene and (9) oxalene.

Lattice Models

Lattice Models

- general Hamiltonian in second quantization ($\hat{c}_i^\dagger$ creation, $\hat{c}_j$ annihilation operator)

$$\hat{H} = \sum_{ij} h_{ij}^{(0)} \hat{c}_i^\dagger \hat{c}_j + \frac{1}{2} \sum_{ijkl} w_{ijkl} \hat{c}_i^\dagger \hat{c}_j^\dagger \hat{c}_l \hat{c}_k$$

- Pariser–Parr–Pople (PPP) Hamiltonian (J hopping, U on-site, V_{ij} long-range interaction)

$$\hat{H} = \underbrace{\underbrace{\underbrace{\sum_{i,\sigma} \epsilon_i \hat{c}_{i,\sigma}^\dagger \hat{c}_{i,\sigma} - J \sum_{\langle i,j \rangle,\sigma} \hat{c}_{i,\sigma}^\dagger \hat{c}_{j,\sigma}}_{\text{Hückel / tight binding}} + U \sum_i \hat{n}_{i,\uparrow} \hat{n}_{i,\downarrow}}_{\text{Hubbard}} + \frac{1}{2} \sum_{i \neq j,\sigma,\sigma'} V_{ij} \left(\hat{n}_{i,\sigma} - 1\right) \left(\hat{n}_{j,\sigma'} - 1\right)}_{\text{PPP}}$$

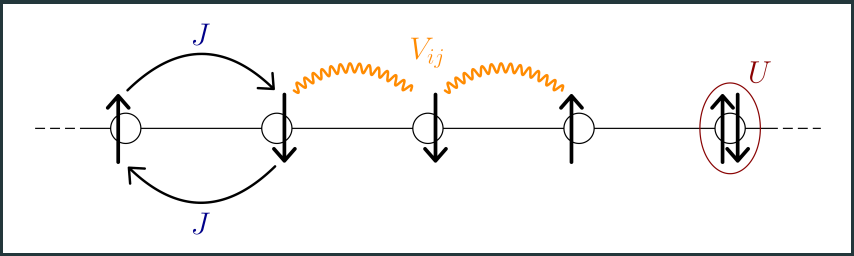

Tight-Binding Model. Geometry-dependent density of states

- tight-binding Hamiltonian

$$\hat{H} = -J \sum_{\langle i,j \rangle, \sigma} \hat{c}^{\dagger}_{i,\sigma} \hat{c}_{j,\sigma}$$

- single fit parameter J
- determined by fit to DFT band structure
- for pristine graphene $J = 2.7\,\mathrm{eV}$

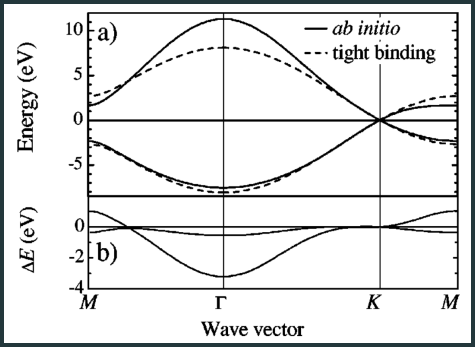

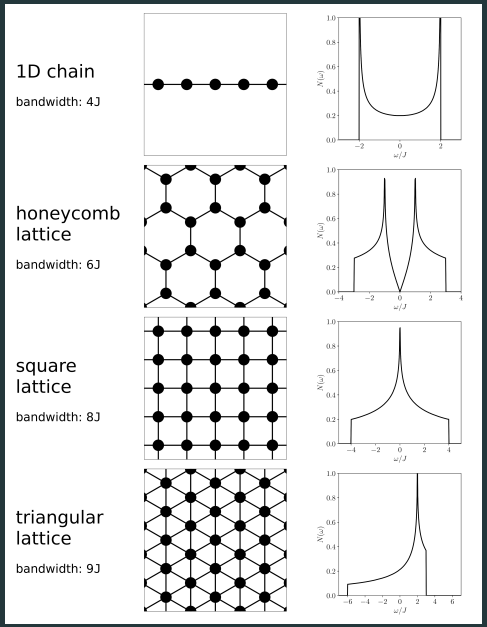

Hubbard Model. Correlations. Band gap

- Hubbard Hamiltonian

$$\hat{H} = -J \sum_{\langle i,j \rangle, \sigma} \hat{c}^{\dagger}_{i,\sigma} \hat{c}_{j,\sigma} + U \sum_{i} \hat{n}_{i,\uparrow} \hat{n}_{i,\downarrow}$$

- local on-site interaction U
- band gap above critical U_c (depends on geometry)
- interaction for graphene strongly depends on system geometry
  - pristine graphene $U \approx 1.6J$
  - nanoribbons $U \approx 3.5J$
- missing long-range interactions have to be compensated by stronger local interaction

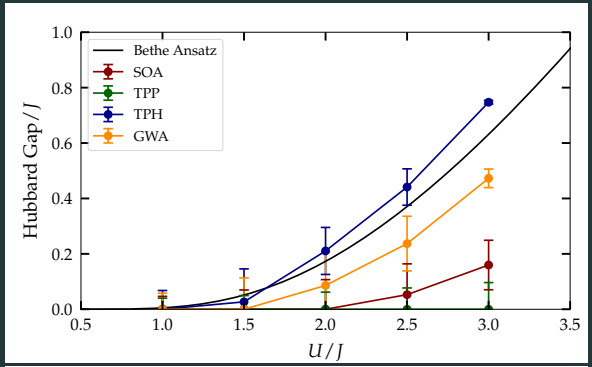

The Pariser–Parr–Pople Model

- Pariser–Parr–Pople Hamiltonian

$$\hat{H} = \sum_{i,\sigma} \epsilon_i \hat{c}^\dagger_{i,\sigma} \hat{c}_{i,\sigma} - J \sum_{\langle i,j\rangle,\sigma} \hat{c}^\dagger_{i,\sigma} \hat{c}_{j,\sigma} + U \sum_i \hat{n}_{i,\uparrow} \hat{n}_{i,\downarrow} + \frac{1}{2} \sum_{i \neq j,\sigma,\sigma'} V_{ij} \left(\hat{n}_{i,\sigma} - 1\right) \left(\hat{n}_{j,\sigma'} - 1\right)$$

- typical parameters for graphene systems less volatile

Parameter	3H-$C_{13}H_9$	$C_{12}H_{10}$	C_6H_6	C_2H_4	$C_{14}H_{10}$
J/eV	2.34	2.39	2.54	2.92	2.4
ϵ_0/J	−3.25	−3.41	–	–	–
U/J	3.54	3.62	3.96	3.61	4.69

- ground-state energy of the Hubbard and PPP dimer:

$$E^{\mathrm{HU}} = \frac{U}{2} - \frac{1}{2}\sqrt{U^2 + 16J^2}$$

$$E^{\mathrm{PPP}} = \frac{U-V}{2} - \frac{1}{2}\sqrt{(U-V)^2 + 16J^2}$$

- U: on-site interation
  V: nearest-neighbor interaction

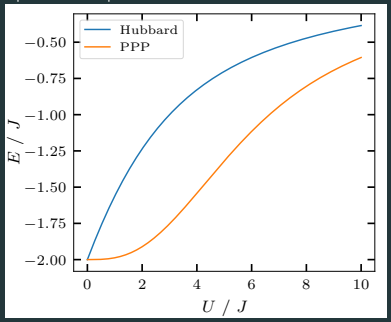

Long-Range Interactions

- long-range interactions given by parametrization (interpolation formula):

$$V_{ij} = U\left[1 + \left(\frac{UR_{ij}}{k_e}\right)^n\right]^{-\frac{1}{n}}$$

- Mataga-Nishimoto ($n = 1$):

$$V_{ij} = U\left[1 + \frac{UR_{ij}}{k_e}\right]^{-1}$$

- Ohno ($n = 2$):

$$V_{ij} = U\left[1 + \left(\frac{UR_{ij}}{k_e}\right)^2\right]^{-\frac{1}{2}}$$

- U in eV, R_{ij} in Å, k_e Coulomb constant

- $\lim_{R_{ij}\to 0} V_{ij} = U$, $\lim_{R_{ij}\to\infty} V_{ij} = \frac{k_e}{R_{ij}}$

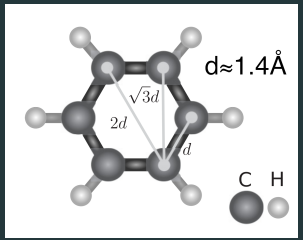

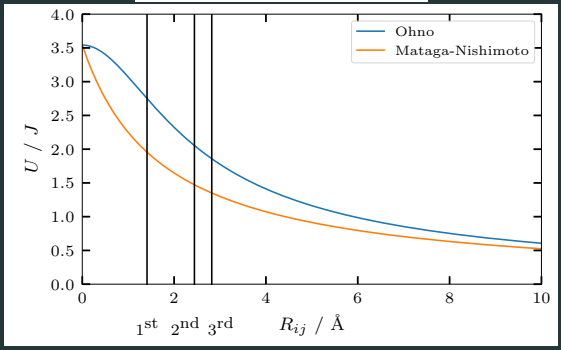

Equilibrium Green Functions

Equilibrium Green Functions Approach to Graphene Nanostructures

Christian-Albrechts-Universität zu Kiel
Mathematisch-Naturwissenschaftliche Fakultät

Dyson equation:

$$G^{\mathrm{R/A}}(\omega) = G_0^{\mathrm{R/A}}(\omega) + G_0^{\mathrm{R/A}}(\omega)\Sigma^{\mathrm{R/A}}(\omega)G^{\mathrm{R/A}}(\omega)$$

Selfconsistent scheme:

0) Initialize $G^{\mathrm{R/A}}(\omega) = G_0^{\mathrm{R/A}}(\omega)$
1) Calculate $G^{\gtrless}(\omega)$ from $G^{\mathrm{R/A}}(\omega)$
2) Perform FFT for $G^{\gtrless}(\omega)$: $\omega \to t$
3) Calculate $\Sigma^{\gtrless}(t)$ and $\Sigma^{\mathrm{R/A}}(t)$
4) Perform FFT for $\Sigma^{\mathrm{R/A}}(t)$: $t \to \omega$
5) Solve Dyson equation for $G^{\mathrm{R/A}}(\omega)$

iterate until convergence

Example: GW self-energy

Diagrammatic representation:

Advantages:

- summation of polarization-bubble diagrams
- moderate- to strong-coupling approximation
- accurate around half filling
- scaling: $\mathcal{O}(N_b^3 \cdot N_\omega \log(N_\omega))$

K. Balzer and M. Bonitz, Lecture Notes Phys. **867**, (2013)

N. Schlünzen, J.-P. Joost *et al.*, Phys. Rev. B **95**, 165139 (2017)

Local density of states of graphene nanoribbons: Bulk vs. End

Christian-Albrechts-Universität zu Kiel
Mathematisch-Naturwissenschaftliche Fakultät

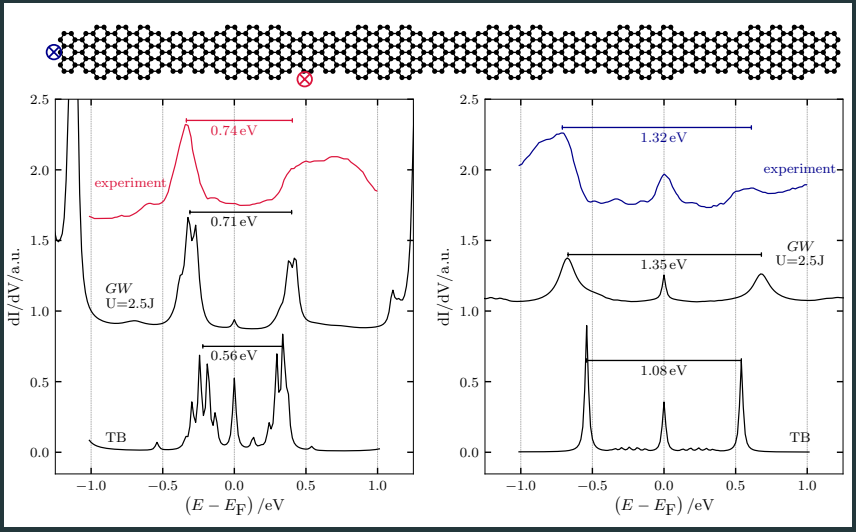

Experiments: Rizzo et al. Nature, **560**, 204 (2018): topological states at the edges and at hetero-junctions
NEGF-GW-Hubbard simulations of 6 unit cells (768 atoms): Joost, Jauho, Bonitz, Nano Lett. **19**, 9045 (2019)
Failure of tight binding and Hartree-Fock results. Electronic correlations crucial for topological states

Multiple ground state solutions. “Löwdin’s symmetry dilemma”[5]

Dyson equation:

$$G^{\mathrm{R/A}}(\omega) = G_0^{\mathrm{R/A}}(\omega) + G_0^{\mathrm{R/A}}(\omega)\Sigma^{\mathrm{R/A}}(\omega)G^{\mathrm{R/A}}(\omega)$$

Do NEGF simulations produce a Hubbard gap (as CI does)? Yes and No!

- SOA yields (at least) 3 ground states
- 1. uniform simulation: no gap, large E
- 2. restricted spin: small gap, lower E
- 3. No restriction: accurate gap, best E
- Allowing symmetry violations improves ground state energy and DOS
- Generalization of Löwdin’s Hartree-Fock result (P. Lykos, G. W. Pratt, RMP 1963)

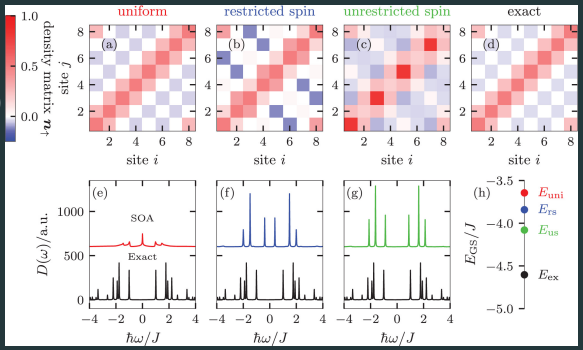

Figure 1: Ground-state properties of a periodic, half-filled Hubbard chain of length L = 8 and U = 4 J, within SOA. (a)–(d) Density matrix for a translationally invariant system (red), without imposing homogeneity but spin symmetry (blue), without both (green), and exact (CI solution without restrictions, black). (e)–(g) DOS, (h) Total ground-state energy for the three cases, compared to the exact result

[5] J.-P. Joost, M. Bonitz, C. Verdozzi *et al.*, Contrib. Plasma Phys. **62**, e202000220 (2021)

Nonequilibrium Green Functions (NEGF)

Nonequilibrium Green Functions (NEGF)

Second quantization

- Fock space $\mathcal{F} \ni |n_1, n_2 \ldots\rangle$, $\quad \mathcal{F} = \bigoplus_{N_0 \in \mathbb{N}} \mathcal{F}^{N_0}$, $\quad \mathcal{F}^{N_0} \subset \mathcal{H}^{N_0}$
- $\hat{c}_i, \hat{c}_i^\dagger$ creates/annihilates a particle in single-particle orbital ϕ_i
- spin accounted for by canonical (anti-)commutation relations
  $\left[\hat{c}_i^{(\dagger)}, \hat{c}_j^{(\dagger)}\right]_\mp = 0, \quad \left[\hat{c}_i, \hat{c}_j^\dagger\right]_\mp = \delta_{i,j}$
- Hamiltonian: $\hat{H}(t) = \underbrace{\sum_{k,m} h^0_{km} \hat{c}_k^\dagger \hat{c}_m}_{\hat{H}_0} + \underbrace{\frac{1}{2} \sum_{k,l,m,n} w_{klmn}(t)\, \hat{c}_k^\dagger \hat{c}_l^\dagger \hat{c}_n \hat{c}_m}_{\hat{W}} + \hat{F}(t)$

Particle interaction $w_{klmn}(t)$

- Coulomb interaction
- electronic correlations (adiabatic switch-on)

Time-dependent excitation $\hat{F}(t)$

- single-particle type
- em field, quench, particle impact etc.

Nonequilibrium Green Functions (contd.)

two times $z, z' \in \mathcal{C}$ ("Keldysh contour"), arbitrary one-particle basis $|\phi_i\rangle$

$$\boxed{G_{ij}(z,z') = \tfrac{\mathrm{i}}{\hbar}\left\langle \hat{T}_{\mathcal{C}} \hat{c}_i(z) \hat{c}_j^\dagger(z') \right\rangle}$$

average with $\hat{\rho}_N$ (unperturbed)
pure or mixed state

Keldysh–Kadanoff–Baym equations (KBE) on $\mathcal{C}$ (2×2 matrix):

$$\sum_k \left\{ \mathrm{i}\hbar \frac{\partial}{\partial z} \delta_{ik} - h_{ik}(z) \right\} G_{kj}(z,z') = \delta_{\mathcal{C}}(z,z')\delta_{ij} - \mathrm{i}\hbar \sum_{klm} \int_{\mathcal{C}} \mathrm{d}\bar{z}\, w_{iklm}(z^+,\bar{z}) G^{(2)}_{lmjk}(z,\bar{z};z',\bar{z}^+)$$

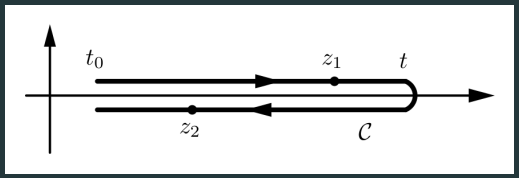

KBE: first equation of Martin–Schwinger hierarchy for $G, G^{(2)} \ldots G^{(n)}$ [and adjoint equation]

- $w\, G^{(2)} \longleftrightarrow \int_{\mathcal{C}} \Sigma\, G$, Selfenergy Σ
- Nonequilibrium Diagram technique
  Example: Hartree–Fock + Second Born selfenergy

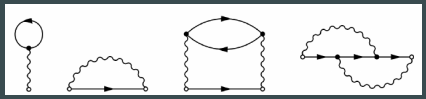

Nonequilibrium: Real-Time Keldysh–Kadanoff–Baym Equations (KBE)

Christian-Albrechts-Universität zu Kiel
Mathematisch-Naturwissenschaftliche Fakultät

- Correlation functions $G^{\gtrless}$ obey real-time KBE

$$\sum_l \left[\mathrm{i}\hbar\frac{\mathrm{d}}{\mathrm{d}t}\delta_{i,l} - h^{\mathrm{eff}}_{il}(t)\right] G^{>}_{lj}(t,t') = I^{(1),>}_{ij}(t,t')\,,$$

$$\sum_l G^{<}_{il}(t,t')\left[-\mathrm{i}\hbar\frac{\overleftarrow{\mathrm{d}}}{\mathrm{d}t'}\delta_{l,j} - h^{\mathrm{eff}}_{lj}(t')\right] = I^{(2),<}_{ij}(t,t')\,,$$

with the effective single-particle **Hartree–Fock Hamiltonian**

$$h^{\mathrm{eff}}_{ij}(t) = h^{0}_{ij} \pm \mathrm{i}\hbar\sum_{kl} w^{\pm}_{ikjl} G^{<}_{lk}(t)$$

and the collision integrals

$$I^{(1),>}_{ij}(t,t') \coloneqq \sum_l \int_{t_\mathrm{s}}^{\infty} \mathrm{d}\bar{t}\left\{\Sigma^{\mathrm{R}}_{il}(t,\bar{t})G^{>}_{lj}(\bar{t},t') + \Sigma^{>}_{il}(t,\bar{t})G^{\mathrm{A}}_{lj}(\bar{t},t')\right\},$$

$$I^{(2),<}_{ij}(t,t') \coloneqq \sum_l \int_{t_\mathrm{s}}^{\infty} \mathrm{d}\bar{t}\left\{G^{\mathrm{R}}_{il}(t,\bar{t})\Sigma^{<}_{lj}(\bar{t},t') + G^{<}_{il}(t,\bar{t})\Sigma^{\mathrm{A}}_{lj}(\bar{t},t')\right\}.$$

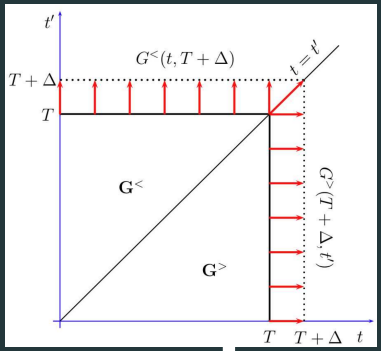

$\mathcal{O}(N_\mathrm{t}^3)$

- numerically demanding due to N_t^3 scaling, but direct access to spectral observables

Conserving nonequilibrium selfenergy approximations[6]

Accuracy depends on coupling strength, density (filling)

Hartree–Fock (HF, mean field): $\sim w^1$

Second Born (2B): $\sim w^2$

GW: ∞ bubble summation, dynamical screening effects

particle-particle T-matrix (TPP): ∞ ladder sum in pp channel

particle-hole T-matrix (TPH/TEH): ∞ ladder sum in ph channel

3rd order approx. (TOA): $\sim w^3$

dynamically screened ladder (DSL)*: $\sim \mathrm{2B} + GW + \mathrm{TPP} + \mathrm{TPH}$

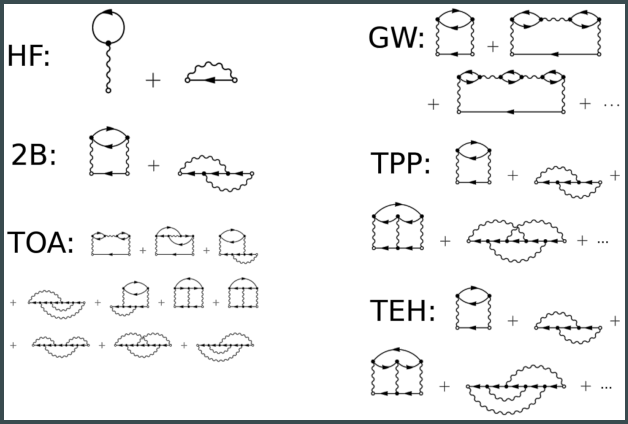

[6] tested against experiment, CI, DMRG: Schlünzen *et al.*, Phys. Rev. B **95**, 165139 (2017)
Review: Schlünzen *et al.*, J. Phys. Cond. Matt. **32**, 103001 (2020); *Joost *et al.*, PRB, 165155 (2022)

Conserving nonequilibrium selfenergy approximations[7]

Christian-Albrechts-Universität zu Kiel
Mathematisch-Naturwissenschaftliche Fakultät

Hartree–Fock (HF, mean field): $\sim w^1$

Second Born (2B): $\sim w^2$

GW: ∞ bubble summation, dynamical screening effects

particle-particle T-matrix (TPP): ∞ ladder sum in pp channel

particle-hole T-matrix (TPH/TEH): ∞ ladder sum in ph channel

3rd order approx. (TOA): $\sim w^3$

dynamically screened ladder (DSL)*: $\sim \mathrm{2B} + GW + \mathrm{TPP} + \mathrm{TPH}$

Accuracy depends on coupling strength, density (filling)

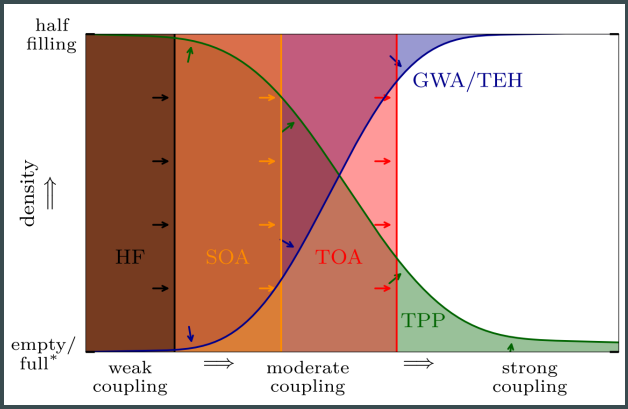

[7] tested against experiment, CI, DMRG: Schlünzen *et al.*, Phys. Rev. B **95**, 165139 (2017)
Review: Schlünzen *et al.*, J. Phys. Cond. Matt. **32**, 103001 (2020); *Joost *et al.*, PRB, 165155 (2022)

Acceleration 1: the GKBA

Acceleration: Generalized Kadanoff–Baym Ansatz (GKBA)[8]

- originally for uniform systems (k - momentum)
- full propagation on the time diagonal ($I := I^<$):

$$\mathrm{i}\hbar\frac{\mathrm{d}}{\mathrm{d}t}G_k^<(t) = \left[h^{\mathrm{HF}}, G^<\right]_k(t) + \left[I + I^\dagger\right]_k(t)$$

- reconstruct off-diagonal NEGF from time diagonal:

$$G_k^{\gtrless}(t,t') = \pm G_k^{\mathrm{R}}(t,t')\rho_k^{\gtrless}(t') + \int_{t'}^{t} dt_1 \int_{-\infty}^{t'} dt_2$$
$$G_k^R(t,t_1)\left[\Sigma_k^R(t_1,t_2)G_k^{\gtrless}(t_2,t') + \Sigma_k^{\gtrless}(t_1,t_2)G_k^A(t_2,t')\right]$$
$$\text{for } t > t', \quad \text{with} \quad \rho_k^{\gtrless}(t) = \pm\mathrm{i}\hbar G_k^{\gtrless}(t,t)$$

- applied to optically excited semiconductors [6], laser plasmas, introducing gauge-invariant GKBA [7]
- quality of GKBA tested in [6], see figure

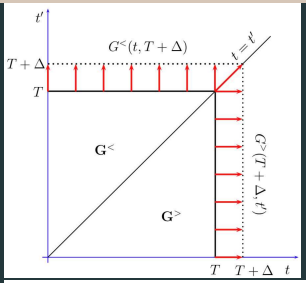

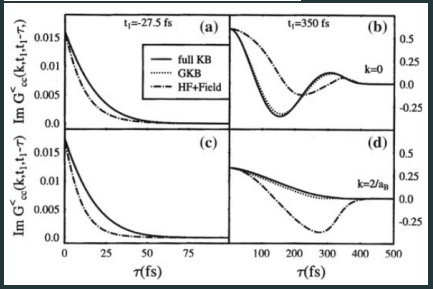

[5] P. Lipavský, V. Špička, and B. Velický, Phys. Rev. B **34**, 6933 (1986);
[6] M. Bonitz *et al.*, J. Phys. Cond. Matt. **8**, 6057 (1996); N.H. Kwong *et al.*, phys. stat. sol. (b) **206**, 197 (1998)
[7] D. Kremp, Th. Bornath, M. Bonitz, and M. Schlanges, Phys. Rev. E **60**, 4725 (1999)

Acceleration: Generalized Kadanoff–Baym Ansatz (contd.)[9]

- **2012: first application to inhomogeneous systems [7]**

$$\mathrm{i}\hbar\frac{\mathrm{d}}{\mathrm{d}t}G^{<}_{ij}(t) = \left[h^{\mathrm{HF}}, G^{<}\right]_{ij}(t) + \left[I + I^{\dagger}\right]_{ij}(t)$$

- reconstruct off-diagonal NEGF from time diagonal:

$$G^{\gtrless}_{ij}(t,t') = \pm\left[G^{\mathsf{R}}_{ik}(t,t')\rho^{\gtrless}_{kj}(t') - \rho^{\gtrless}_{ik}(t)G^{\mathsf{A}}_{kj}(t,t')\right]$$

$$\text{with} \quad \rho^{\gtrless}_{ij}(t) = \pm\mathrm{i}\hbar G^{\gtrless}_{ij}(t,t)$$

- HF-GKBA: use Hartree–Fock propagators for $G^{\mathsf{R/A}}_{ij}$

$$G^{\mathsf{R/A}}_{ij}(t,t') = \mp\mathrm{i}\Theta\left(\pm[t-t']\right)\exp\left(-\frac{\mathrm{i}}{\hbar}\int_{t'}^{t}\mathrm{d}\bar{t}\,h_{\mathrm{HF}}(\bar{t})\right)\Big|_{ij}$$

- conserves total energy
- applications to atoms, molecules, 2D quantum materials

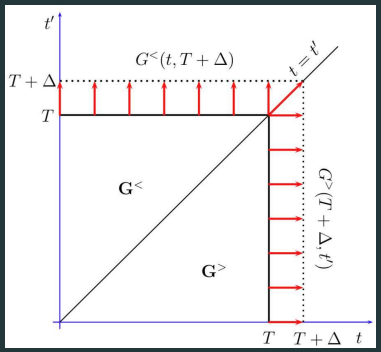

$$\mathcal{O}(N_{\mathrm{t}}^2)$$

[6] P. Lipavský, V. Špička, and B. Velický, Phys. Rev. B **34**, 6933 (1986);
[7] S. Hermanns, K. Balzer, and M. Bonitz, Phys. Scr. **2012,** 014036 (2012); K. Balzer and M. Bonitz, Lecture Notes in Physics **867** (2013)

Application of the Generalized Kadanoff–Baym Ansatz

- G. Stefanucci, R. van Leeuwen, Y. Pavlyukh, C. Verdozzi, A. Marini, and co-workers and many others
- atoms, molecules, quantum materials
- memory truncation[a]
- long-time limit, transition to Boltzmann-type equations, retardation expansion[b]
- transition from reversible to irreversible transport equations[c]

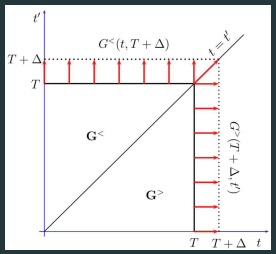

[a] W. Schäfer and M. Wegener, *Semiconductor Optics and Transport Phenomena*, Springer 2002, talk by M. Eckstein

[b] M. Bonitz, *Quantum Kinetic Theory*, Teubner 1998

[c] Bonitz, Scharnke, Schlünzen, Contrib. Plasma Phys. **58**, 1036 (2018)

Acceleration 2: the G1–G2 scheme

Reformulating the GKBA

- quadratic/cubic scaling is caused by the structure of the collision integral

$$I_{ij}(t) = \sum_k \int_{t_0}^{t} \mathrm{d}\bar{t} \left[\Sigma^{>}_{ik}(t,\bar{t}) G^{<}_{kj}(\bar{t},t) - \Sigma^{<}_{ik}(t,\bar{t}) G^{>}_{kj}(\bar{t},t) \right] =: \pm \mathrm{i}\hbar \sum_{klp} w_{iklp}(t) \mathcal{G}_{lpjk}(t)$$

- example 2nd Born selfenergy:[10]

$$\Sigma^{\gtrless}_{ij}\left(t,t'\right) = \pm \left(\mathrm{i}\hbar\right)^2 \sum_{klpqrs} w_{iklp}\left(t\right) w^{\pm}_{qrjs}\left(t'\right) G^{\gtrless}_{lq}\left(t,t'\right) G^{\gtrless}_{pr}\left(t,t'\right) G^{\lessgtr}_{sk}\left(t',t\right)$$

- correlated part $\mathcal{G}(t)$ of 2-particle NEGF identified as

$$\mathcal{G}_{ijkl}(t) = \mathrm{i}\hbar \sum_{pqrs} \int_{t_0}^{t} \mathrm{d}\bar{t}\, w^{\pm}_{pqrs}\left(\bar{t}\right) \left[\mathcal{G}^{\mathsf{H},>}_{ijpq}(t,\bar{t}) \mathcal{G}^{\mathsf{H},<}_{rskl}(\bar{t},t) - \mathcal{G}^{\mathsf{H},<}_{ijpq}(t,\bar{t}) \mathcal{G}^{\mathsf{H},>}_{rskl}(\bar{t},t) \right]$$

  with the two-particle Hartree Green function

$$\mathcal{G}^{\mathsf{H},\gtrless}_{ijkl}(t,t') := G^{\gtrless}_{ik}(t,t') G^{\gtrless}_{jl}(t,t')$$

[10] N. Schlünzen, J.-P. Joost and M. Bonitz, Phys. Rev. Lett. **124**, 076601 (2020)

Reformulating the GKBA (contd.)

- two-particle SOA-$\mathcal{G}$ in HF-GKBA with initial correlations

$$\mathcal{G}_{ijkl}(t) - \mathcal{G}_{ijkl}(t_0) = (\mathrm{i}\hbar)^3 \sum_{pqrs} \int_{t_0}^{t} \mathrm{d}\bar{t}\, \mathcal{U}^{(2)}_{ijpq}(t,\bar{t}) \Psi^{\pm}_{pqrs}(\bar{t}) \mathcal{U}^{(2)}_{rskl}(\bar{t},t)$$

with the single-time source term (no longer depends on the outer time)

$$\Psi^{\pm}_{ijkl}(t) = (\mathrm{i}\hbar)^2 \sum_{pqrs} w^{\pm}_{pqrs}(t) \left[\mathcal{G}^{\mathsf{H},>}_{ijpq}(t,t) \mathcal{G}^{\mathsf{H},<}_{rskl}(t,t) - \mathcal{G}^{\mathsf{H},<}_{ijpq}(t,t) \mathcal{G}^{\mathsf{H},>}_{rskl}(t,t) \right]$$

and the two-particle Hartree–Fock time-evolution operators obeying Schrödinger-type EOMs

$$\frac{\mathrm{d}}{\mathrm{d}t} \left[\mathcal{U}^{(2)}_{ijkl}(t,\bar{t}) \right] = \frac{1}{\mathrm{i}\hbar} \sum_{pq} h^{(2),\mathsf{HF}}_{ijpq}(t) \mathcal{U}^{(2)}_{pqkl}(t,\bar{t})$$

$$\frac{\mathrm{d}}{\mathrm{d}t} \left[\mathcal{U}^{(2)}_{ijkl}(\bar{t},t) \right] = -\frac{1}{\mathrm{i}\hbar} \sum_{pq} \mathcal{U}^{(2)}_{ijpq}(\bar{t},t) h^{(2),\mathsf{HF}}_{pqkl}(t)$$

with the effective two-particle Hamiltonian

$$h^{(2),\mathsf{HF}}_{ijkl}(t) = \delta_{jl} h^{\mathsf{HF}}_{ik}(t) + \delta_{ik} h^{\mathsf{HF}}_{jl}(t)$$

Time-linear NEGF simulations: the G1–G2 Scheme[11]

- full propagation on the time diagonal, as for ordinary HF-GKBA:

$$\mathrm{i}\hbar\frac{\mathrm{d}}{\mathrm{d}t}G^{<}_{ij}(t) = \left[h^{\mathrm{HF}}, G^{<}\right]_{ij}(t) + \left[I + I^{\dagger}\right]_{ij}(t)$$

- but collision integral defined by correlated two-particle Green function

$$I_{ij}(t) = \pm\mathrm{i}\hbar\sum_{klp} w_{iklp}(t)\mathcal{G}_{lpjk}(t)$$

$\mathcal{O}(N_{\mathrm{t}}^1)$

- which obeys an ordinary (time-local) differential equation

$$\mathrm{i}\hbar\frac{\mathrm{d}}{\mathrm{d}t}\mathcal{G}_{ijkl}(t) = \left[h^{(2),\mathrm{HF}}, \mathcal{G}\right]_{ijkl}(t) + \Psi^{\pm}_{ijkl}(t)$$

- two initial values:

$$G^{0,<}_{ij} = \pm\frac{1}{\mathrm{i}\hbar}n_{ij}(t_0) =: \pm\frac{1}{\mathrm{i}\hbar}n^0_{ij}\,,$$
$$\mathcal{G}^0_{ijkl} = \frac{1}{(\mathrm{i}\hbar)^2}\left\{n^0_{ijkl} - n^0_{ik}n^0_{jl} \mp n^0_{il}n^0_{jk}\right\}\,,$$

  i.e. density matrix and pair correlations existing in the system at the initial time $t = t_0$
  Correlated initial state generated by adiabatic switching, starting from $\mathcal{G} = 0$.

[11] N. Schlünzen, J.-P. Joost, and M. Bonitz, Phys. Rev. Lett. **124**, 076601 (2020)

Extending the G1–G2 Scheme to T-matrix or/and GW selfenergies

- other selfenergy approximations can be reformulated in the G1–G2 scheme in similar fashion:[12]

$$\mathrm{i}\hbar\frac{\mathrm{d}}{\mathrm{d}t}\mathcal{G}_{ijkl}(t) = \left[h^{(2),\mathsf{HF}}(t),\mathcal{G}(t)\right]_{ijkl} + \Psi^{\pm}_{ijkl}(t) + \underbrace{L_{ijkl}(t)}_{\text{TPP}} + \underbrace{P_{ijkl}(t)}_{GW} \pm \underbrace{P_{jikl}(t)}_{\text{TPH}}$$

$$L_{ijkl} \coloneqq \sum_{pq}\left\{\mathfrak{h}^{L}_{ijpq}\mathcal{G}_{pqkl} - \mathcal{G}_{ijpq}\left[\mathfrak{h}^{L}_{klpq}\right]^{*}\right\}, \qquad \mathfrak{h}^{L}_{ijkl} \coloneqq (\mathrm{i}\hbar)^2\sum_{pq}\left[\mathcal{G}^{\mathsf{H},>}_{ijpq} - \mathcal{G}^{\mathsf{H},<}_{ijpq}\right] w_{pqkl}\,,$$

$$P_{ijkl} \coloneqq \sum_{pq}\left\{\mathfrak{h}^{\Pi}_{qjpl}\mathcal{G}_{piqk} - \mathcal{G}_{qjpl}\left[\mathfrak{h}^{\Pi}_{qkpi}\right]^{*}\right\}, \qquad \mathfrak{h}^{\Pi}_{ijkl} \coloneqq \pm(\mathrm{i}\hbar)^2\sum_{pq} w^{\pm}_{qipk}\left[\mathcal{G}^{\mathsf{F},>}_{jplq} - \mathcal{G}^{\mathsf{F},<}_{jplq}\right]$$

and the Hartree/Fock (H/F) two-particle Green functions

$$\mathcal{G}^{\mathsf{H},\gtrless}_{ijkl}(t) \coloneqq G^{\gtrless}_{ik}(t,t)G^{\gtrless}_{jl}(t,t)\,, \qquad \mathcal{G}^{\mathsf{F},\gtrless}_{ijkl}(t) \coloneqq G^{\gtrless}_{il}(t,t)G^{\lessgtr}_{jk}(t,t)$$

- Dynamically-screened-ladder (DSL) approximation: TPP + GW + TPH diagrams. No explicit selfenergy known.[13] Nonequilibrium generalization of ground state results (Bethe-Salpeter equation, Wang-Cassing or Valdemoro approximation, $\mathcal{G}^3 = 0$)

[12] J.-P. Joost, N. Schlünzen, and M. Bonitz, PRB **101**, 245101 (2020), Joost *et al.*, PRB **105**, 165155 (2022)

[13] J.-P. Joost, PhD thesis, Kiel University 2023

Extending the G1–G2 Scheme to T-matrix or/and GW selfenergies

C | A | U
Christian-Albrechts-Universität zu Kiel
Mathematisch-Naturwissenschaftliche Fakultät

- G1–G2 scheme recovers conserving selfenergy approximations but contains more options[14]
- Exchange diagrams require special treatment (second lines)

approximation	G1–G2 notation	Selfenergy
SOA	Ψ^0	Σ^{SOA}
	$\Psi^\pm$	$\Sigma^{\mathrm{SOA}} + \Sigma_x^{\mathrm{SOA}}$
TPP	$\Psi^0 + L^0$	Σ^{TPP}
	$\Psi^\pm + L$	$\Sigma^{\mathrm{TPP}} + \Sigma_x^{\mathrm{TPP}}$
GW	$\Psi^0 + \Pi^0$	Σ^{GW}
	$\Psi^\pm + \Pi^\pm$	–
DSL	$\Psi^0 + \Pi^0 + L^0$	–
	$\Psi^\pm + \Pi^\pm + L$	–
TOA	$\Psi^\pm + \Pi^\pm[G_2^{\mathrm{SOA}}] +$ $+ L[G_2^{\mathrm{SOA}}]$	Σ^{TOA}

Table 1: Correspondence of many-body approximations of Green functions (correlation selfenergies) and reduced density operators (terms in the $\mathcal{G}_2$-equation) and their defining equations

[14] J.-P. Joost, N. Schlünzen, and M. Bonitz, PRB **101**, 245101 (2020), Joost *et al.*, PRB **105**, 165155 (2022)

Numerical Scaling of G1–G2 vs. Standard HF-GKBA

- time-linear scaling achieved quickly. Dramatic gain compared to ordinary HF-GKBA
- Complex selfenergies: little overhead to SOA. Example: 10-site Hubbard chain

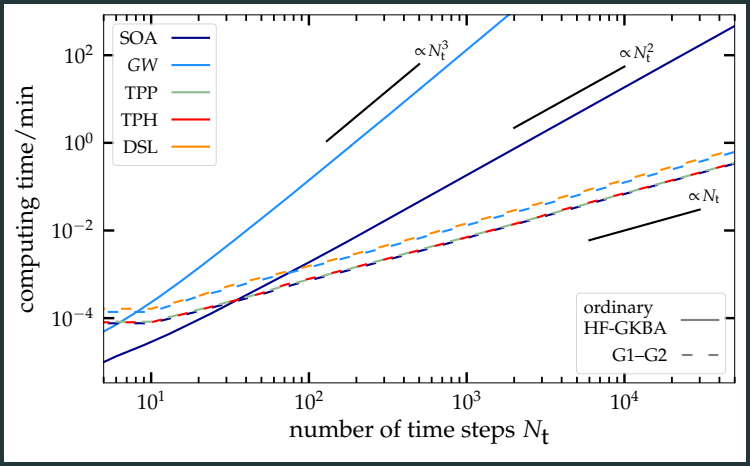

CPU time of G1–G2: dependence on Basis type and dimension N_b

Basis		SOA	GW	TPP	DSL
general	G1–G2 CPU time	$N_\mathrm{b}^5 N_\mathrm{t}$	$N_\mathrm{b}^6 N_\mathrm{t}$	$N_\mathrm{b}^6 N_\mathrm{t}$	$N_\mathrm{b}^6 N_\mathrm{t}$
w_{ijkl}	speedup vs HF-GKBA	N_t	N_t^2	N_t^2	–
Hubbard	G1–G2 CPU time	$N_\mathrm{b}^4 N_\mathrm{t}$	$N_\mathrm{b}^4 N_\mathrm{t}$	$N_\mathrm{b}^4 N_\mathrm{t}$	$N_\mathrm{b}^4 N_\mathrm{t}$
U	speedup vs HF-GKBA	$N_\mathrm{t}/N_\mathrm{b}$	$N_\mathrm{t}^2/N_\mathrm{b}$	$N_\mathrm{t}^2/N_\mathrm{b}$	–
jellium	G1–G2 CPU time	$N_\mathrm{b}^3 N_\mathrm{t}$	$N_\mathrm{b}^3 N_\mathrm{t}$	$N_\mathrm{b}^4 N_\mathrm{t}$	$N_\mathrm{b}^4 N_\mathrm{t}$
$\tilde{w}(q)$	speedup vs HF-GKBA	N_t	N_t^2	$N_\mathrm{t}^2/N_\mathrm{b}$	–

- largest speedup against HF-GKBA: general basis and jellium
- Hubbard: basis size disadvantage, but still huge gain
- DSL impossible with standard HF-GKBA or 2-time NEGF

CPU time of G1–G2: dependence on Basis type and dimension N_b

Basis		SOA	GW	TPP	DSL
general	G1–G2 CPU time	$N_\mathrm{b}^5 N_\mathrm{t}$	$N_\mathrm{b}^6 N_\mathrm{t}$	$N_\mathrm{b}^6 N_\mathrm{t}$	$N_\mathrm{b}^6 N_\mathrm{t}$
w_{ijkl}	speedup vs HF-GKBA	N_t	N_t^2	N_t^2	–
$\mathcal{G}_{ijkl}$	G1–G2 RAM	N_b^4	N_b^4		
Hubbard	G1–G2 CPU time	$N_\mathrm{b}^4 N_\mathrm{t}$	$N_\mathrm{b}^4 N_\mathrm{t}$	$N_\mathrm{b}^4 N_\mathrm{t}$	$N_\mathrm{b}^4 N_\mathrm{t}$
U	speedup vs HF-GKBA	$N_\mathrm{t}/N_\mathrm{b}$	$N_\mathrm{t}^2/N_\mathrm{b}$	$N_\mathrm{t}^2/N_\mathrm{b}$	–
$\mathcal{G}_{ijkl}$	G1–G2 RAM	N_b^4			
jellium	G1–G2 CPU time	$N_\mathrm{b}^3 N_\mathrm{t}$	$N_\mathrm{b}^3 N_\mathrm{t}$	$N_\mathrm{b}^4 N_\mathrm{t}$	$N_\mathrm{b}^4 N_\mathrm{t}$
$\tilde{w}(q)$	speedup vs HF-GKBA	N_t	N_t^2	$N_\mathrm{t}^2/N_\mathrm{b}$	–
$\mathcal{G}_{\vec{p}_1,\vec{p}_2,\vec{q}}$	G1–G2 RAM	$N_\mathrm{b}^{3\cdot d}$	$N_\mathrm{b}^{3\cdot d}$		

Drawbacks of G1–G2 scheme:

- large RAM for storage of instantaneous $\mathcal{G}$ (e.g. jellium only possible in 1D[15])
- propagation of two not fully independent equations (trace consistency between G_1 and G_2)
  $\Rightarrow$ possible way around: quantum fluctuations approach (talk of Erik Schroedter)[16]
- possible instabilities for long times and/or strong coupling (requires regularization)

[15] C. Makait, F. Borges-Fajardo, and M. Bonitz, Contrib. Plasma Phys. e202300008 (2023)

[16] E. Schroedter, J.-P. Joost, and M. Bonitz, Cond. Matt. Phys. **25**, 23401 (2022)

Instabilities and regularization ("purification")

- instability related to violation of N-representability [Coleman, Maziotti] and of trace consistency [also discussed by Akbari, van Leeuwen *et al.*, PRB 2012]
- formal source: positive eigenvalues, $0 < \lambda \leq \lambda_{\max}$, of two-particle Green function
- problem similar to positive definiteness of spectral functions [Stefanucci, van Leeuwen *et al.*]
- "purification" procedure and trace consistency restoration: Lackner *et al.*, PRA 2015, 2017 and J.-P. Joost, PhD thesis, Kiel 2022
- Open questions remain

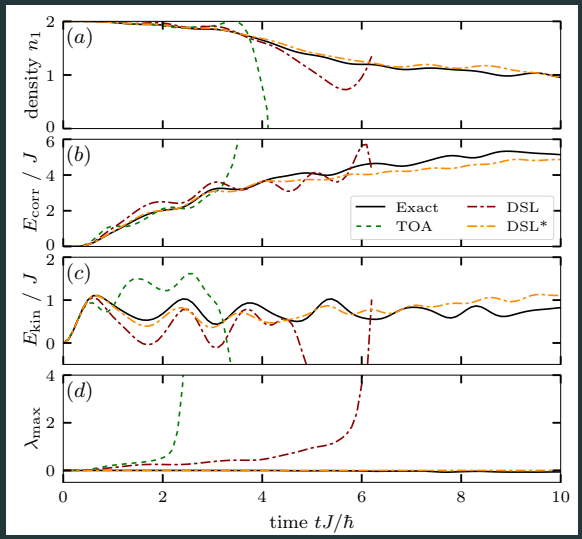

6-site Hubbard chain at half filling, $U/J = 4$, initially sites 1–3 doubly occupied, $t = 0$: confinement quench [Joost *et al.*, PRB **105**, 165155 (2022)]

Nonequilibrium dynamics of 2D quantum materials

Excitation of Topological Edge States[17]

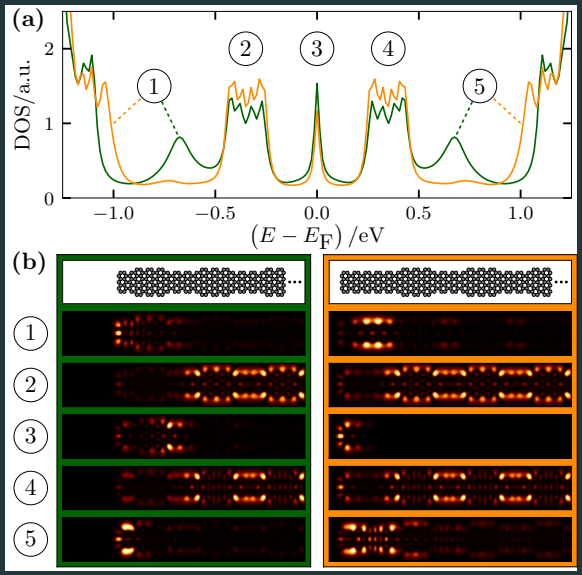

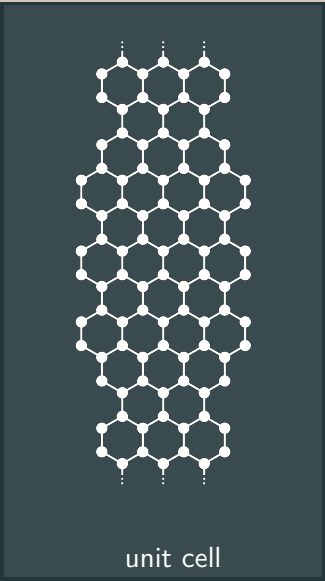

[17] J.-P. Joost, A.-P. Jauho, and M. Bonitz, Nano Lett. **19**, 9045 (2019)

Nonequilibrium G1–G2 simulations for GNR

- one unit cell with 96 lattice sites
- nonequilibrium dynamics using the G1–G2 scheme with DSL + purification
- 96 lattices sites just fit in the memory of a V100 GPU on the CAU-NEC cluster (for now largest system we can consider)
- propagation time not an issue due to linear scaling

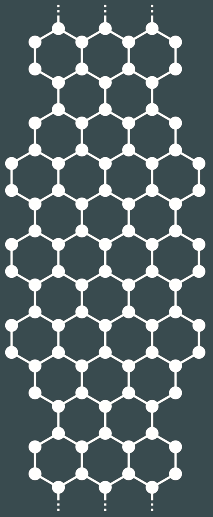

unit cell

DOS and Edge States of the Unit Cell using Equilibrium GW[18]

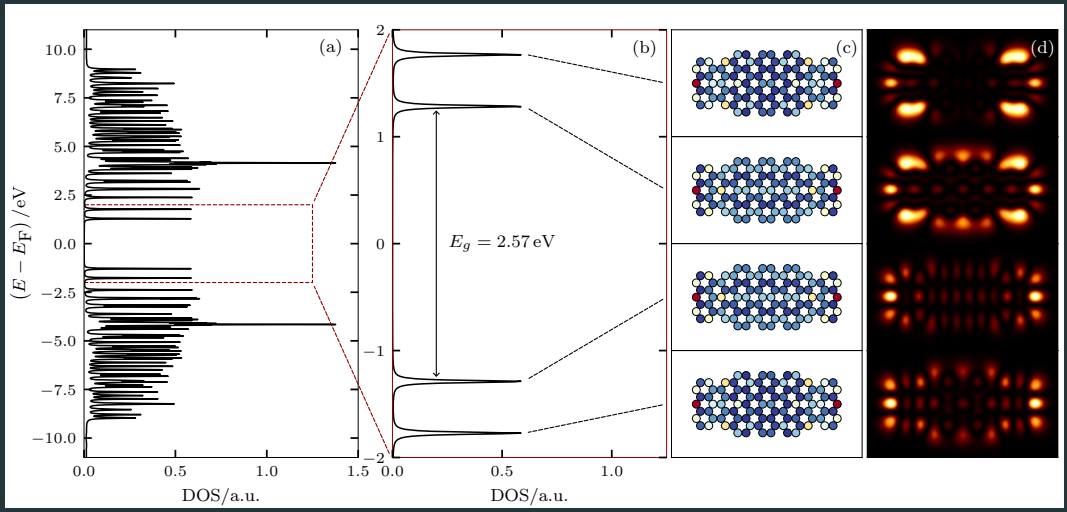

[18] J.-P. Joost, PhD thesis, Kiel University 2022

Laser Excitation in the G1–G2 Scheme

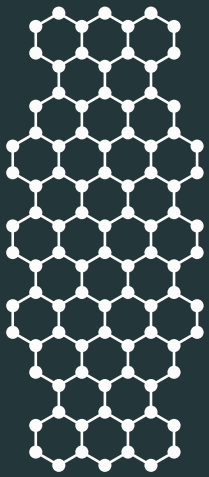

Laser parameters

- dipole approx. (wavelength μm, system nm)
- $U_{\text{pot}} = -\vec{E}_{\text{Laser}} \cdot \vec{x}$
- $E_{\text{Laser}} = E_0 \exp\left(-\frac{(t-t_0)^2}{2\sigma_L^2}\right)$
- $E_0 = (6-60)\, V/\mu m$
- $\omega_L = (0.1-3.0) J \approx (0.2-7.0)\,\text{eV}$
- $\sigma_L = 10 J^{-1} \approx 3\,\text{fs}$
- fluence $F = (0.9-122)\, mJ/cm^2$
- polarizations: $\parallel, \perp, \circlearrowleft$

Idea: try site-selective excitation (topological states), even though laser field (nearly) uniform across GNR [J.-P. Joost, PhD thesis, Kiel University 2022]

Short-Time Carrier Dynamics[19]

$\|, E_0 = 6\,V/\mu m,\ \omega_L = 1.2\text{eV}\,(\text{IR})$

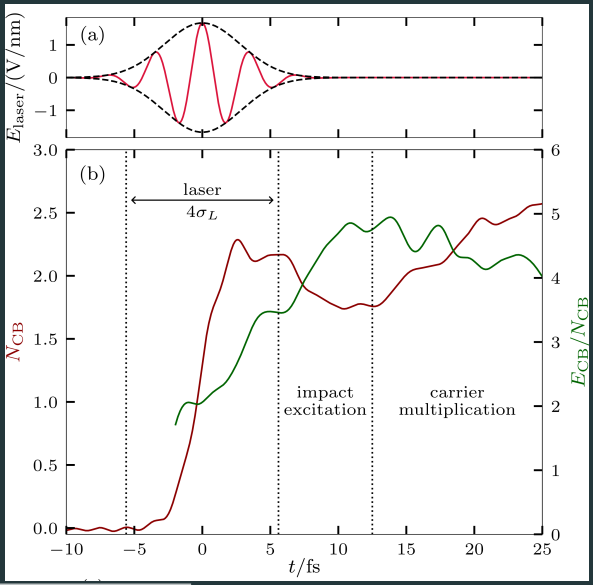

[19] J.-P. Joost, PhD thesis, Kiel University 2022

Local Occupation of Excited Electrons[20] $\|, E_0 = 6\,V/\mu m,\ \omega_L = 1.2\text{eV}$

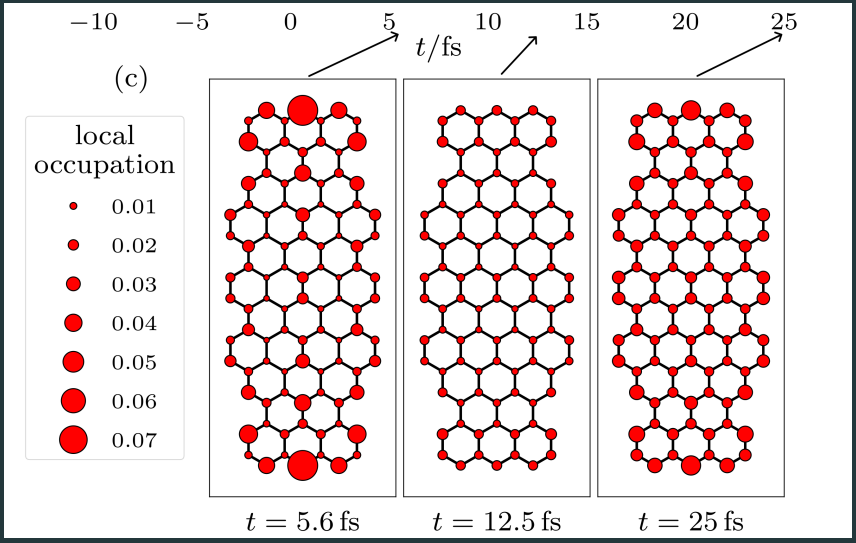

[20] J.-P. Joost, PhD thesis, Kiel University 2022

$\|, E_0 = 6\,V/\mu m,\ \omega_L = 1.2\text{eV}\,(\text{IR})$

Christian-Albrechts-Universität zu Kiel
Mathematisch-Naturwissenschaftliche Fakultät

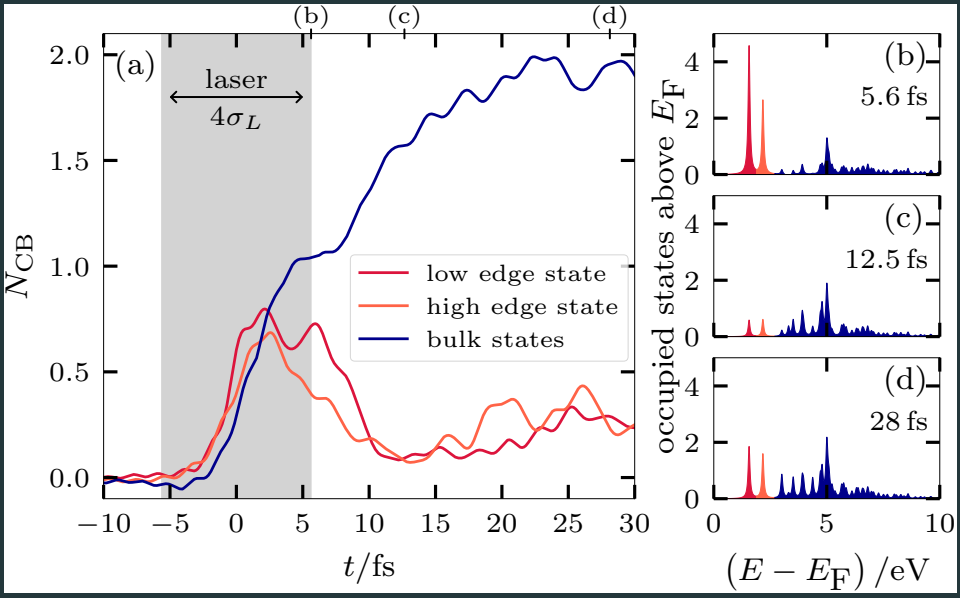

Femtosecond response of quantum materials to ion impact[21]

- of interest for plasma-surface interaction, e.g. Kiel CRC initiative of J. Benedikt
- Extreme cases: experiments with highly charged ions at TU Vienna (R. Wilhelm)
- Xe^{Z+} ion penetrates monolayers of graphene and MoS_2, $Z = 20 \ldots 40$
- ultrafast emission of slow electrons into vacuum: $\sim 20 \ldots 80$ electrons per ion!
- complex charge transfer: interatomic Coulomb decay (Auger-type process)

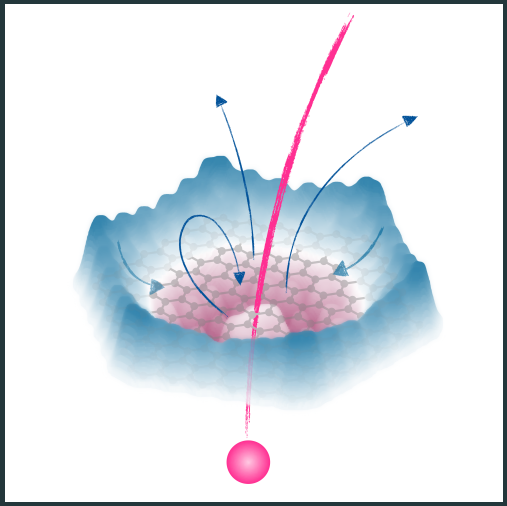

[21] A. Niggas *et al.*, Phys. Rev. Lett. **129**, 086802 (2022), Editors' Choice

Electron emission as sensitive diagnostic of quantum materials[22]

- Experiment: same ion causes emission of 7 times more electrons from graphene (SLG) than from MoS_2 (QF: target support)
- Ion acts as sensitive probe of the material with single-site resolution
- theoretical explanation requires sub-femtosecond resolution of electronic correlations

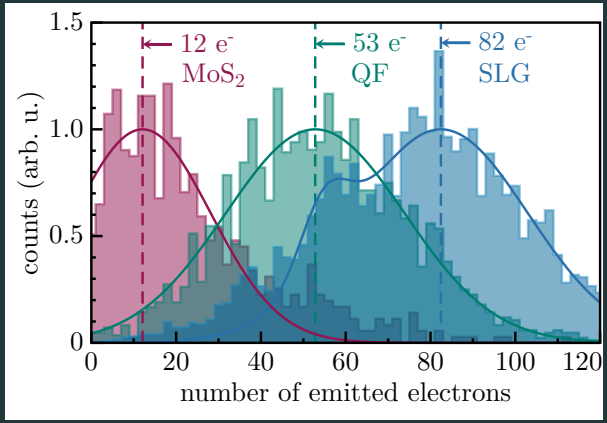

[22] A. Niggas *et al.*, Phys. Rev. Lett. **129**, 086802 (2022), Editors' Choice

NEGF embedding scheme. Fast time-local formulation[23]

[23] K. Balzer, N. Schlünzen, H. Ohldag, J.-P. Joost, and M. Bonitz, Phys. Rev. B **107**, 155141 (2023)

NEGF-approach to open systems: embedding scheme

Idea: Physical system (s) embedded in ("large") environment (e) that is treated in simplified manner

I. Standard Thermodynamic approach: Averaging over degrees of freedom of environment, loss of information (Zubarev, Lindblad and others): $\hat{\rho}_s = \mathrm{Tr}_e \hat{\rho}_{s+e}$, no access to dynamics of "e"

II. NEGF embedding idea: No averaging. Dynamical approach to system and environment plus coupling. Typically, "e" is treated as non-interacting, e.g. *Stefanucci, van Leeuwen* book. Examples:

- electron transport between leads (= environment, e)
- ionization of atoms (continuum state = e), Covito *et al.*
- resonant charge transfer between ion (= e) impacting target,
  Bonitz *et al.*, Front. Chem. Sciences Engin. **13**, 201-237 (2019);
  model for highly charged ions: Balzer and Bonitz, CPP **62**, e202100041 (2021)

NEGF formulation:

$$\Omega = \{s, e\}: \qquad H_{\text{total}} = \sum_{\alpha\beta\in\Omega} \sum_{ij} h_{ij}^{\alpha\beta}(t) c_i^{\alpha\dagger} c_j^{\beta} + \frac{1}{2} \sum_{\alpha\beta\gamma\delta\in\Omega} \sum_{ijkl} w_{ijkl}^{\alpha\beta\gamma\delta} c_i^{\alpha\dagger} c_j^{\beta\dagger} c_k^{\gamma} c_l^{\delta} \,.$$

$$\text{NEGF, density matrix}: \quad G_{ij}^{\alpha\beta}(t,t') = -\mathrm{i}\langle T_C c_i^{\alpha}(t) c_j^{\beta\dagger}(t')\rangle \,, \qquad \rho_{ij}^{\alpha\beta}(t) = -\mathrm{i} G_{ji}^{\beta\alpha}(t,t^+) \,,$$

$$\text{Short notation}: \quad G_{ij}^{\alpha\alpha}(t,t') \to G_{ij}^{\alpha}(t,t')$$

Standard 2-time NEGF embedding scheme

Approximations: neglect correlations in environment and s-e coupling: $\Sigma^e \to 0$, $\Sigma^{se} \to 0$

Keldysh-Kadanoff-Baym equations of total system including coupling (se) terms:

$$\left\{\mathrm{i}\partial_t \delta_{ik} - h^{\mathrm{HF,s}}_{ik}(t)\right\} G^{\mathrm{s}}_{kj}(t,t') = h^{\mathrm{HF,se}}_{i\underline{k}}(t) G^{\mathrm{es}}_{\underline{k}\,j}(t,t') + \delta_{ij}\delta_C(t,t') + \int_C \mathrm{d}\bar{t}\, \Sigma^{\mathrm{s}}_{ik}(t,\bar{t}) G^{\mathrm{s}}_{kj}(\bar{t},t')\,. \tag{1}$$

$$\left\{\mathrm{i}\partial_t \delta_{\underline{i}\underline{k}} - h^{\mathrm{HF,e}}_{\underline{i}\underline{k}}(t)\right\} G^{\mathrm{es}}_{\underline{k}\,j}(t,t') = h^{\mathrm{HF,es}}_{\underline{i}k}(t) G^{\mathrm{s}}_{kj}(t,t')\,, \tag{2}$$

$$\left\{\mathrm{i}\partial_t \delta_{\underline{i}\underline{k}} - h^{\mathrm{HF,e}}_{\underline{i}\underline{k}}(t)\right\} g^{\mathrm{e}}_{\underline{k}\underline{j}}(t,t') = \delta_{\underline{i}\underline{j}}\delta_C(t,t')\,. \tag{3}$$

Idea: rewrite effect of environment as additional selfenergy for G^s: Eq. (3) defines inverse GF: $\sum_{\underline{k}} \int_C d\bar{t}\, g^{e,-1}_{\underline{i}\underline{k}}(t,\bar{t}) g^{e}_{\underline{k}\underline{j}}(\bar{t},t') = \delta_{\underline{i}\underline{j}}\delta_C(t,t')$, with the results:

$$g^{e,-1}_{\underline{i}\underline{k}}(t,\bar{t}) = \left\{\mathrm{i}\partial_t \delta_{\underline{i}\underline{k}} - h^{\mathrm{HF,e}}_{\underline{i}\underline{k}}(t)\right\}\delta_C(t,\bar{t})\,, \qquad G^{\mathrm{es}}_{\underline{k}\,j}(t,t') = \int_C d\bar{t}\, g^{\mathrm{e}}_{\underline{k}\underline{j}}(t,\bar{t}) h^{\mathrm{HF,es}}_{\underline{i}k}(\bar{t}) G^{\mathrm{s}}_{kj}(\bar{t},t')\,,$$

$$h^{\mathrm{HF,se}}_{i\underline{k}}(t) G^{\mathrm{es}}_{\underline{k}\,j}(t,t') = \int_C d\bar{t}\, \Sigma^{\mathrm{emb}}_{il}(\bar{t},t') G^{\mathrm{s}}_{lj}(t,t')\,, \quad \text{eliminate } G^{\mathrm{es}} \text{ from (1)}$$

$$\Sigma^{\mathrm{emb}}_{ij}(t,t') = \sum_{\underline{k}\underline{l}} h^{\mathrm{HF,se}}_{i\,\underline{k}}(t) g^{\mathrm{e}}_{\underline{k}\,\underline{l}}(t,t') h^{\mathrm{HF,es}}_{\underline{l}\,j}(t')\,, \qquad h^{\mathrm{HF,se}}_{i\underline{j}}(t) = \int \mathrm{d}^3 r\, \phi^{\mathrm{s}*}_i(\vec{r})(\hat{T} + \hat{V}^{\mathrm{HF}}) \chi^{\mathrm{e}}_{\underline{j}}(\vec{r};t)\,.$$

$\Rightarrow$ retain closed equation (1) for system NEGF with total selfenergy $\Sigma^S + \Sigma^{\mathrm{emb}}$

Application to ion impact: resonant charge transfer and charge buildup

Christian-Albrechts-Universität zu Kiel
Mathematisch-Naturwissenschaftliche Fakultät

- NEGF simulations by Karsten Balzer (216 sites)
- initially all lattice sites half filled (uncharged, 4 bands)
- ion attracts electrons towards impact point (center), depletion of outer honeycombs
- resonant charge transfer from innermost ring to ion (red arrow)
- strongly differing induced potential in both materials
- emitted electrons (via ICD) will be accelerated away from SLG, but attracted back to MoS_2, explaining findings in experiment

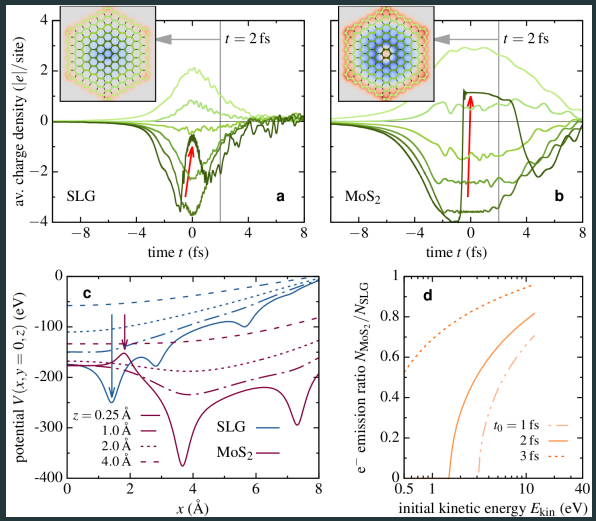

[24] A. Niggas *et al.*, Phys. Rev. Lett. **129**, 086802 (2022), Editors' Choice

Nonequilibrium Electron energy spectrum during ion impact[25]

- G1–G2 simulations by Niclas Schlünzen applying Koopmans' theorem (without charge transfer)
- significantly stronger excitation of electrons in graphene than in MoS_2 [-1fs: just before charge transfer]
- reproduces experimental trends of different number of ionized electrons despite similar work functions
- Reason for different material behaviors: higher electron mobility and larger bandwidth of SLG
- but: so far only TDHF simulations

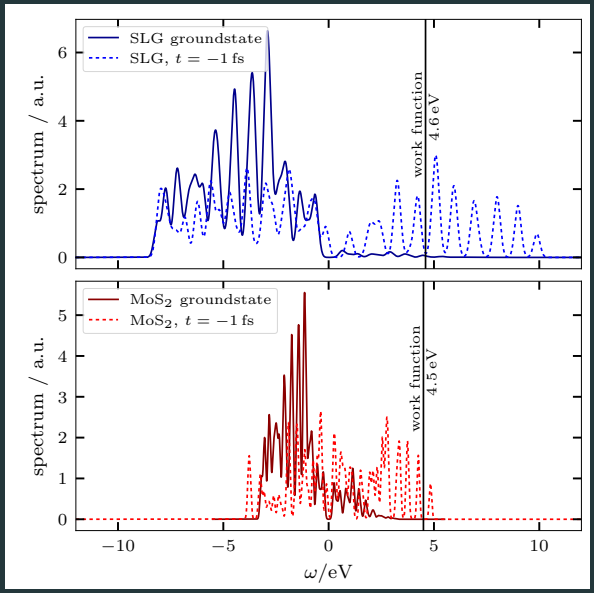

[25] A. Niggas *et al.*, Phys. Rev. Lett. **129**, 086802 (2022), Editors' Choice

Acceleration: Time-local embedding scheme. G1–G2 equations[27]

Equation for $G^{s<}$ on time diagonal:

$$\mathrm{i}\partial_t G^{s<}_{ij}(t) - \left[h^{\mathrm{HF,s}}, G^{<}\right]^{s}_{ij,t} = \left(I(t) + I^{\dagger}(t)\right)_{ij}\,, \quad I_{ij}(t) = I^{\mathrm{cor}}_{ij}(t) + I^{\mathrm{emb}}_{ij}(t)\,, \tag{4}$$

$$I_{ij}(t) = \int_{t_0}^{t} \mathrm{d}\bar{t}\left\{\Sigma^{>}_{ik}(t,\bar{t})G^{s<}_{kj}(\bar{t},t) - \Sigma^{<}_{ik}(t,\bar{t})G^{s>}_{kj}(\bar{t},t)\right\}\,, \quad \Sigma^{\gtrless} = \Sigma^{cor,\gtrless} + \Sigma^{\mathrm{emb},\gtrless} \tag{5}$$

Apply Hartree-Fock-GKBA:

$$G^{\gtrless}_{ij}(t,t') = \mathrm{i}\left[G^{\mathrm{R}}_{ik}(t,t')G^{\gtrless}_{kj}(t') - G^{\gtrless}_{ik}(t)G^{\mathrm{A}}_{kj}(t,t')\right], \tag{6}$$

Time differentiation of I^{cor} yields equation for 2-particle NEGF [26] (example second Born approx.):

$$\mathrm{i}\partial_t \mathcal{G}_{ijkl}(t) - \left[h^{(2),\mathsf{HF}}(t), \mathcal{G}(t)\right]_{ijkl} = \Psi^{\pm}_{ijkl}(t)\,, \tag{7}$$

$$h^{(2),\mathsf{HF}}_{ijkl}(t) = h^{\mathsf{HF}}_{ik}(t)\delta_{jl} + h^{\mathsf{HF}}_{jl}(t)\delta_{ik}\,, \qquad \mathcal{G}^{\mathsf{H},\gtrless}_{ijkl}(t) \coloneqq G^{\gtrless}_{ik}(t,t)G^{\gtrless}_{jl}(t,t)\,, \tag{8}$$

$$\Psi^{\pm}_{ijkl}(t) = \mathrm{i}^2 \sum_{pqrs} w^{\pm}_{pqrs}(t)\left\{\mathcal{G}^{\mathsf{H},>}_{ijpq}\mathcal{G}^{\mathsf{H},<}_{rskl} - (>\leftrightarrow<)\right\}_t\,, \tag{9}$$

[26] Schluenzen et al., Phys. Rev. Lett. **124**, 076601 (2020)

[27] Balzer et al., Phys. Rev. B **107**, 155141 (2023)

Time-local embedding scheme. G1–G2 equations (contd.)[28]

Equation for $G^{s<}$ on time diagonal contains additional "embedding" collision integral:

$$\mathrm{i}\partial_t G^{s<}_{ij}(t) - \left[h^{\mathrm{HF},s}, G^{<}\right]^{s}_{ij,t} = \left(I(t) + I^{\dagger}(t)\right)_{ij}, \quad I_{ij}(t) = I^{\mathrm{cor}}_{ij}(t) + I^{\mathrm{emb}}_{ij}(t), \tag{10}$$

$$I_{ij}(t) = \int_{t_0}^{t} \mathrm{d}\bar{t}\left\{\Sigma^{>}_{ik}(t,\bar{t})G^{s<}_{kj}(\bar{t},t) - \Sigma^{<}_{ik}(t,\bar{t})G^{s>}_{kj}(\bar{t},t)\right\}, \quad \Sigma^{\gtrless} = \Sigma^{cor,\gtrless} + \Sigma^{\mathrm{emb},\gtrless} \tag{11}$$

Time differentiation of $I^{\mathrm{emb}} = h^{\mathrm{HF,se}}G^{\mathrm{se},<}$ yields equation for charge transfer NEGF, $\mathrm{G}^{\mathrm{es},<}$:

$$G^{\mathrm{es},<}_{\underline{i}\,j}(t) = \int_{t_0}^{t} \mathrm{d}\bar{t}\, h^{\mathrm{HF,es}}_{\underline{k}\,l}(\bar{t})\left[g^{\mathrm{e},>}_{\underline{i}\,\underline{k}}(t,\bar{t})G^{s,<}_{lj}(\bar{t},t) - g^{\mathrm{e},<}_{\underline{i}\,\underline{k}}(t,\bar{t})G^{s,>}_{lj}(\bar{t},t)\right].$$

$$\mathrm{i}\frac{\mathrm{d}}{\mathrm{d}t}G^{\mathrm{es},<}_{\underline{i}\,j}(t) - \left(h^{\mathrm{HF,e}}G^{\mathrm{es},<}\right)^{\mathrm{e}}_{\underline{i}\,j,t} + \left(G^{\mathrm{es},<}h^{\mathrm{HF},s}\right)^{\mathrm{s}}_{\underline{i}\,j,t} = \left(h^{\mathrm{HF,es}}G^{s,<}\right)^{\mathrm{s}}_{\underline{i}\,j,t} - \left(g^{\mathrm{e},<}h^{\mathrm{HF,es}}\right)^{\mathrm{e}}_{\underline{i}\,j,t}.$$

$$\mathrm{i}\frac{\mathrm{d}}{\mathrm{d}t}g^{\mathrm{e},<}_{\underline{i}\,\underline{j}}(t) = \left[h^{\mathrm{HF,e}}g^{\mathrm{e},<}\right]^{\mathrm{e}}_{\underline{i}\,\underline{j},t}, \qquad (AB)^{s,e}_{ij,t} = \sum_{k\in s,e} A_{ik}(t)B_{kj}(t),$$

[28] Balzer *et al.*, Phys. Rev. B **107**, 155141 (2023)

Numerical test: charge transfer between a Hubbard chain + 1 site

Hubbard chain ($i = 1 \dots L$) with Hartree interaction, $\langle \hat{n}_i^{\mathsf{s}} \rangle(t) = -\mathrm{i} G_{ii}^{\mathsf{s},<}(t)$

$$h_{ij}^{\mathsf{HF,s}}(t) = -J\delta_{\langle i,j\rangle} + \delta_{ij}\, U \left(\langle \hat{n}_i^{\mathsf{s}} \rangle(t) - \frac{1}{2} \right) ,$$

time-dependent charge transfer to site "0"

$$h_{i0}^{\mathsf{se}}(t) = \delta_{i1}\, \gamma_0 \cdot e^{-(t-t_\gamma)^2/2\tau_\gamma^2} , \quad t_0 = J^{-1}$$

K. Balzer and M. Bonitz, Contrib. Plasma Phys. **62** (2021)

Figure for $L = 6$ and three s-e couplings γ_0

black line: charge transfer pulse
full lines: two-time embedding scheme
dotted lines: present G1–G2 scheme
unexpected failure for large γ_0!

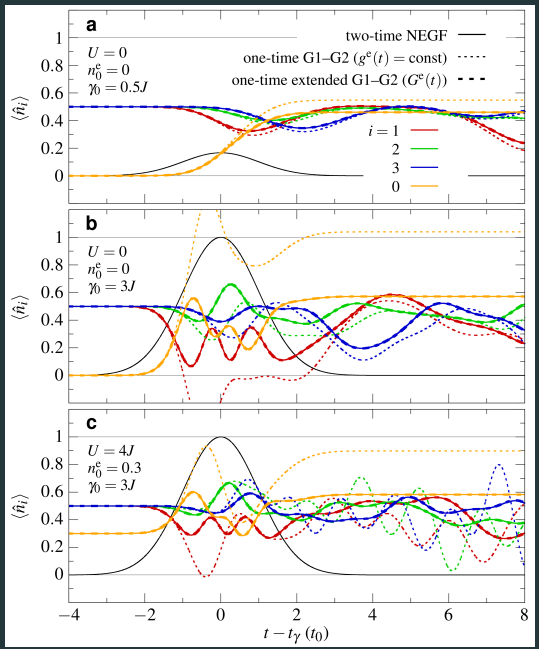

What is wrong with the time-local embedding scheme?

- for large charge transfer amplitude γ_0, simulations yield negative site occupations, occupation of target site ("environment") exceeds 1
- occurs already for the simplest case (correlations turned off)
- the original NEGF simulations have built in conservation laws (energy, particle number) and spin statistics (Pauli principle)
- the HF-GKBA (and the G1-G2 scheme) do not violate conservation laws
- no problems observed in two-time embedding equations for arbitrary γ_0, exact agreement with KBE for full system

$\Rightarrow$ Need to reconsider treatment of charge transfer in time-local G1–G2 equations.

Extended time-local NEGF embedding scheme[29]

Need to extend the environment equation and the Hartree-Fock-GKBA:

$$\left\{\mathrm{i}\partial_t\delta_{\underline{ik}} - h^{\mathrm{HF,e}}_{\underline{ik}}(t)\right\} G^{\mathrm{e}}_{\underline{kj}}(t,t') = \delta_{\underline{ij}}\delta_C(t,t') + h^{\mathrm{HF,es}}_{\underline{ik}}(t) G^{\mathrm{se}}_{\underline{kj}}(t,t') \tag{12}$$

$$\begin{aligned} G^{\mathrm{s}\gtrless}_{ij}(t,t') = \mathrm{i}\left[G^{\mathrm{sR}}_{ik}(t,t')G^{\mathrm{s}\gtrless}_{kj}(t') - G^{\mathrm{s}\gtrless}_{ik}(t)G^{\mathrm{sA}}_{kj}(t,t')\right] \\ + \mathrm{i}\left[G^{\mathrm{se}R}_{i\underline{k}}(t,t')G^{\mathrm{es}\gtrless}_{\underline{k}j}(t') - G^{\mathrm{se}\gtrless}_{i\underline{k}}(t)G^{\mathrm{es}\mathrm{A}}_{\underline{k}j}(t,t')\right], \end{aligned} \tag{13}$$

Result: extended time-local embedding equations:

$$\mathrm{i}\frac{\mathrm{d}}{\mathrm{d}t}G^{\mathrm{es},<}_{\underline{i}\,j}(t) = \left(h^{\mathrm{HF,es}}G^{\mathrm{s},<}\right)^{\mathrm{s}}_{\underline{i}\,j,t} - \left(G^{\mathrm{e},<}h^{\mathrm{HF,es}}\right)^{\mathrm{e}}_{\underline{i}\,j,t} + \left(h^{\mathrm{HF,e}}G^{\mathrm{es},<}\right)^{\mathrm{e}}_{\underline{i}\,j,t} - \left(G^{\mathrm{es},<}h^{\mathrm{HF,s}}\right)^{\mathrm{s}}_{\underline{i}\,j,t}, \tag{14}$$

$$\mathrm{i}\frac{\mathrm{d}}{\mathrm{d}t}G^{\mathrm{e},<}_{\underline{i}\,\underline{j}}(t) = \left[h^{\mathrm{HF,e}}, G^{\mathrm{e},<}\right]^{\mathrm{e}}_{\underline{i}\,\underline{j},t} + \left(h^{\mathrm{HF,es}}G^{\mathrm{se},<}\right)^{\mathrm{s}}_{\underline{i}\,\underline{j},t} - \left(G^{\mathrm{es},<}h^{\mathrm{HF,se}}\right)^{\mathrm{s}}_{\underline{i}\,\underline{j},t}. \tag{15}$$

Comments:

- Eq. (14) remains unchanged, with substitution $g^e \to G^e$
- Main change: yellow terms in Eq. (15), this restores conservation laws
- Advantage of two-time version of embedding: G^e not needed at all, only g^{e}.

[29] Balzer *et al.*, Phys. Rev. B **107**, 155141 (2023)

Test of the extended time-local embedding scheme

Hubbard chain ($L = 6$) with Hartree interaction, $\langle \hat{n}_i^{\mathsf{s}} \rangle(t) = -\mathrm{i} G_{ii}^{\mathsf{s},<}(t)$

$$h_{ij}^{\mathsf{HF},\mathsf{s}}(t) = -J\delta_{\langle i,j\rangle} + \delta_{ij}\, U \left(\langle \hat{n}_i^{\mathsf{s}} \rangle(t) - \frac{1}{2} \right) ,$$

time-dependent charge transfer to site "0"

$$h_{i0}^{\mathsf{se}}(t) = \delta_{i1}\, \gamma_0 \cdot e^{-(t-t_\gamma)^2/2\tau_\gamma^2} , \quad t_0 = J^{-1}$$

black line: charge transfer pulse
full lines: two-time embedding scheme
dots: standard G1–G2 embedding scheme
extended scheme: dashes
correct[a] for arbitrary γ_0

[a] Balzer *et al.*, Phys. Rev. B **107**, 155141 (2023)

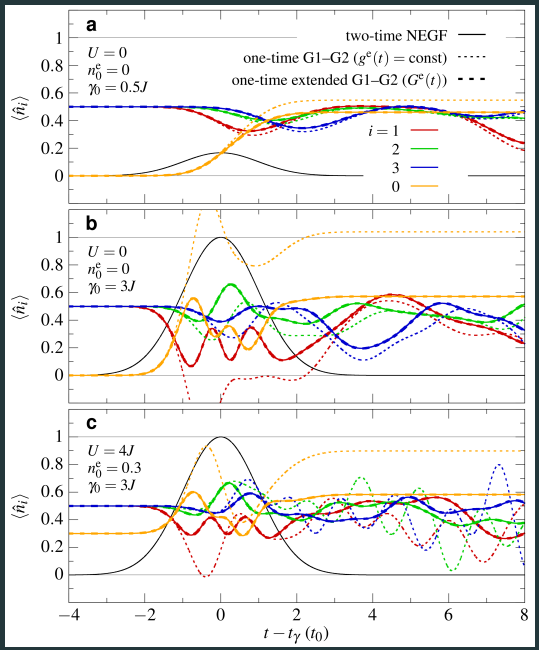

Numerical test: dependence on energy ε of site "0", for $L = 50$

Hubbard chain ($i = 1 \dots L$) with Hartree interaction, $\langle \hat{n}_i^{\mathsf{s}} \rangle(t) = -\mathrm{i} G_{ii}^{\mathsf{s},<}(t)$

$$h_{ij}^{\mathsf{HF},\mathsf{s}}(t) = -J\delta_{\langle i,j\rangle} + \delta_{ij}\, U \left(\langle \hat{n}_i^{\mathsf{s}} \rangle(t) - \frac{1}{2} \right) ,$$

time-dependent charge transfer to site "0"

$$h_{i0}^{\mathsf{se}}(t) = \delta_{i1}\, \gamma_0 \cdot e^{-(t-t_\gamma)^2/2\tau_\gamma^2} , \quad t_0 = J^{-1}$$

Figure for $L = 50$, $\gamma_0 = 2J$

black line: charge transfer pulse
line styles: different U[a]
ε_i: energy of site 0, colors: cases

⇒ Extended embedding scheme preserves all conservation laws and time-linear scaling of the G1–G2 scheme

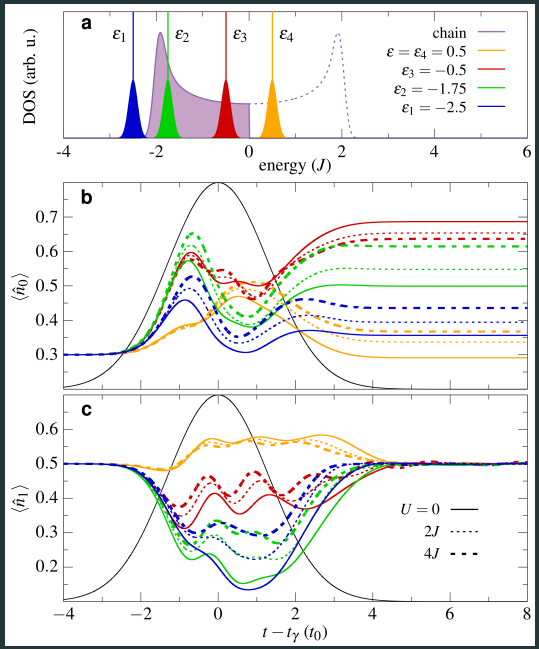

[a] Balzer *et al.*, Phys. Rev. B **107**, 155141 (2023)

Summary and outlook

Summary: Acceleration of NEGF simulations for correlated systems

1. Finite systems
   - 2-time NEGF and HF-GKBA[30] have comparable accuracy, each with pros and cons
   - G1–G2 scheme: exact time-local reformulation of HF-GKBA, speedup $\mathcal{O}(N_t)$ to $\mathcal{O}(N_t^2)$. Full access to pp and ph T-matrix, GW, DSL and 3-particle diagrams[31]
   - long-time stability issues: contraction consistency, "purification"[32]
2. Macroscopic systems
   - 2-time simulations more accurate and stable than GKBA
   - HF-GKBA suffers from aliasing effects. Correlated propagators needed[33]
3. G1–G2 bottleneck: dimension of $\mathcal{G} \sim \mathcal{O}(N_B^4) \rightarrow$ massive parallelization and
   - Quantum fluctuations approach $\rightarrow$ reduction to $\mathcal{O}(N_B^2)$ scaling for GW[34]
   - embedding schemes $\rightarrow$ heterogeneous optimized basis, minimal correlations[35]

[30] S. Hermanns, K. Balzer, and M. Bonitz, Phys. Scr. **2012,** 014036 (2012)
[31] Karlsson, Pavlyukh, Perfetto, Stefanucci, Tuovinen, van Leeuwen,...
[32] J.-P. Joost *et al.*, PRB (2022), Joost, PhD thesis (2022), I. Brezinova *et al.*
[33] M. Bonitz, *Quantum Kinetic Theory*, 2nd ed. Springer 2016
[34] E. Schroedter *et al.*, Cond. Matt. Phys. **25** (2), 23401 (2022)
[35] K. Balzer *et al.*, Phys. Rev. B **107**, 155141 (2023-04-15), Tuovinen *et al.*; PRL **130**, 246301 (2023-06-16)

Outlook 1: NEGF embedding scheme with correlated selfenergies[36]

$$\left\{\mathrm{i}\partial_t\delta_{ik} - h^{\mathrm{HF,s}}_{ik}(t)\right\} G^{\mathrm{s}}_{kj}(t,t') = h^{\mathrm{HF,se}}_{i\,\underline{k}}(t) G^{\mathrm{es}}_{\underline{k}\,j}(t,t') + \delta^{C}_{ij} + \int_C \mathrm{d}\bar{t}\, \Sigma^{\mathrm{s}}_{ik}(t,\bar{t}) G^{\mathrm{s}}_{kj}(\bar{t},t') + \int_C \mathrm{d}\bar{t}\, \Sigma^{\mathrm{se}}_{i\,\underline{k}}(t,\bar{t}) G^{\mathrm{es}}_{\underline{k}j}(\bar{t},t')$$

$$\left\{\mathrm{i}\partial_t\delta_{\underline{i}\,\underline{k}} - h^{\mathrm{HF,e}}_{\underline{i}\,\underline{k}}(t)\right\} G^{\mathrm{e}}_{\underline{k}\,\underline{j}}(t,t') - \int_C \mathrm{d}\bar{t}\, \Sigma^{\mathrm{e}}_{\underline{i}\underline{k}}(t,\bar{t}) G^{\mathrm{e}}_{\underline{k}\underline{j}}(\bar{t},t') = \delta^{C}_{\underline{i}\,\underline{j}} + h^{\mathrm{HF,es}}_{\underline{i}k}(t) G^{\mathrm{se}}_{k\,\underline{j}}(t,t') + \int_C \mathrm{d}\bar{t}\, \Sigma^{\mathrm{es}}_{\underline{i}k}(t,\bar{t}) G^{\mathrm{se}}_{k\underline{j}}(\bar{t},t')$$

$$\left\{\mathrm{i}\partial_t\delta_{\underline{i}\,\underline{k}} - h^{\mathrm{HF,e}}_{\underline{i}\,\underline{k}}(t)\right\} g^{\mathrm{e}}_{\underline{k}\,\underline{j}}(t,t') - \int_C \mathrm{d}\bar{t}\, \Sigma^{\mathrm{e}}_{\underline{i}\underline{k}}(t,\bar{t}) g^{\mathrm{e}}_{\underline{k}\underline{j}}(\bar{t},t') = \delta_{\underline{i}\,\underline{j}}\delta_C(t,t')\,.$$

$$\left\{\mathrm{i}\partial_t\delta_{\underline{i}\,\underline{k}} - h^{\mathrm{HF,e}}_{\underline{i}\,\underline{k}}(t)\right\} G^{\mathrm{es}}_{\underline{k}\,j}(t,t') - \int_C \mathrm{d}\bar{t}\, \Sigma^{\mathrm{e}}_{\underline{i}\underline{k}}(t,\bar{t}) G^{\mathrm{es}}_{\underline{k}j}(\bar{t},t') = h^{\mathrm{HF,es}}_{\underline{i}\,k}(t) G^{\mathrm{s}}_{kj}(t,t') + \int_C \mathrm{d}\bar{t}\, \Sigma^{\mathrm{es}}_{\underline{i}k}(t,\bar{t}) G^{\mathrm{s}}_{kj}(\bar{t},t')\,,$$

Solution for G^{es} and embedding selfenergy, using inverse GF:

$$g^{\mathrm{e}\,-1}_{\underline{i}\,\underline{k}}(t,\bar{t}) = \left[\mathrm{i}\partial_t\delta_{\underline{i}\,\underline{k}} - h^{\mathrm{HF,e}}_{\underline{i}\,\underline{k}}(t)\right]\delta_C(t,\bar{t}) - \Sigma^{\mathrm{e}}_{\underline{i}k}(t,\bar{t})\,,$$

$$G^{\mathrm{es}}_{\underline{l}\,j}(t,t') = \int_C \mathrm{d}\bar{t}\, g^{\mathrm{e}}_{\underline{l}\,\underline{i}}(t,\bar{t})\, h^{\mathrm{HF,es}}_{\underline{i}\,k}(\bar{t})\, G^{\mathrm{s}}_{kj}(\bar{t},t') + \int_C \mathrm{d}\bar{t} \int_C \mathrm{d}\tilde{t}\, g^{\mathrm{e}}_{\underline{l}\,\underline{i}}(t,\bar{t})\, \Sigma^{\mathrm{es}}_{\underline{i}\,k}(\bar{t},\tilde{t})\, G^{\mathrm{s}}_{kj}(\tilde{t},t')\,.$$

$$\Sigma^{\mathrm{emb}}_{ik}(t,\tilde{t}) = \int_C \mathrm{d}\bar{t} \int_C \mathrm{d}\bar{\bar{t}} \left\{h^{\mathrm{HF,se}}_{i\,\underline{k}}(\bar{t})\,\delta_C(t,\bar{t}) + \Sigma^{\mathrm{se}}_{i\,\underline{k}}(t,\bar{t})\right\} g^{\mathrm{e}}_{\underline{l}\,\underline{i}}(\bar{t},\bar{\bar{t}})\, \left\{h^{\mathrm{HF,es}}_{\underline{i}\,k}(\bar{\bar{t}})\,\delta_C(\bar{\bar{t}},\tilde{t}) + \Sigma^{\mathrm{es}}_{\underline{i}\,k}(\bar{\bar{t}},\tilde{t})\right\}\,,$$

[36] M. Bonitz, K. Balzer, H. Ohldag, to be published

Outlook 2: Multi-layer NEGF embedding scheme[37]: $f \to e \to s$

$$\left\{\mathrm{i}\partial_t\delta_{ik} - h^{\mathrm{HF,s}}_{ik}(t)\right\} G^{\mathrm{s}}_{kj}(t,t') = h^{\mathrm{HF,se}}_{i\,\underline{k}}(t) G^{\mathrm{es}}_{\underline{k}\,j}(t,t') + \delta^{C}_{ij} + \int_C \mathrm{d}\bar{t}\, \Sigma^{\mathrm{s}}_{ik}(t,\bar{t}) G^{\mathrm{s}}_{kj}(\bar{t},t') + \int_C \mathrm{d}\bar{t}\, \Sigma^{\mathrm{se}}_{i\underline{k}}(t,\bar{t}) G^{\mathrm{es}}_{\underline{k}j}(\bar{t},t')$$

$$\left\{\mathrm{i}\partial_t\delta_{\underline{i}\,\underline{k}} - h^{\mathrm{HF,e}}_{\underline{i}\,\underline{k}}(t)\right\} G^{\mathrm{e}}_{\underline{k}\,\underline{j}}(t,t') - \int_C \mathrm{d}\bar{t}\, \Sigma^{\mathrm{e}}_{\underline{i}\underline{k}}(t,\bar{t}) G^{\mathrm{e}}_{\underline{k}\underline{j}}(\bar{t},t') = \delta^{C}_{\underline{i}\,\underline{j}} + h^{\mathrm{HF,es}}_{\underline{i}k}(t) G^{\mathrm{se}}_{k\,\underline{j}}(t,t') + \int_C \mathrm{d}\bar{t}\, \Sigma^{\mathrm{es}}_{\underline{i}k}(t,\bar{t}) G^{\mathrm{se}}_{k\underline{j}}(\bar{t},t') + h^{\mathrm{HF,ef}}_{\underline{i}\alpha}(t) G^{\mathrm{fe}}_{\alpha\,\underline{j}}(t,t') + \int_C \mathrm{d}\bar{t}\, \Sigma^{\mathrm{ef}}_{\underline{i}\alpha}(t,\bar{t}) G^{\mathrm{fe}}_{\alpha\underline{j}}(\bar{t},t')$$

$$\left\{\mathrm{i}\partial_t\delta_{\underline{i}\,\underline{k}} - h^{\mathrm{HF,e}}_{\underline{i}\,\underline{k}}(t)\right\} g^{\mathrm{e}}_{\underline{k}\,\underline{j}}(t,t') - \int_C \mathrm{d}\bar{t}\, \tilde{\Sigma}^{\mathrm{e}}_{\underline{i}\underline{k}}(t,\bar{t}) g^{\mathrm{e}}_{\underline{k}\underline{j}}(\bar{t},t') = \delta_{\underline{i}\,\underline{j}}\delta_C(t,t')\,.$$

$$\left\{\mathrm{i}\partial_t\delta_{\underline{i}\,\underline{k}} - h^{\mathrm{HF,e}}_{\underline{i}\,\underline{k}}(t)\right\} G^{\mathrm{es}}_{\underline{k}\,j}(t,t') - \int_C \mathrm{d}\bar{t}\, \tilde{\Sigma}^{\mathrm{e}}_{\underline{i}\underline{k}}(t,\bar{t}) G^{\mathrm{es}}_{\underline{k}j}(\bar{t},t') = h^{\mathrm{HF,es}}_{\underline{i}\,k}(t) G^{\mathrm{s}}_{kj}(t,t') + \int_C \mathrm{d}\bar{t}\, \Sigma^{\mathrm{es}}_{\underline{i}k}(t,\bar{t}) G^{\mathrm{s}}_{kj}(\bar{t},t')$$

$$\left\{\mathrm{i}\partial_t\delta_{\alpha\,\gamma} - h^{\mathrm{HF,f}}_{\alpha\,\gamma}(t)\right\} G^{\mathrm{f}}_{\gamma\beta}(t,t') - \int_C \mathrm{d}\bar{t}\, \Sigma^{\mathrm{f}}_{\alpha\gamma}(t,\bar{t}) G^{\mathrm{f}}_{\gamma\beta}(\bar{t},t') = \delta^{C}_{\alpha\beta} + h^{\mathrm{HF,fe}}_{\alpha\underline{k}} G^{\mathrm{ef}}_{\underline{k}\,\beta}(t,t') + \int_C \mathrm{d}\bar{t}\, \Sigma^{\mathrm{fe}}_{\alpha\underline{k}}(t,\bar{t}) G^{\mathrm{ef}}_{\underline{k}\beta}(\bar{t},t')$$

$$\left\{\mathrm{i}\partial_t\delta_{\alpha\,\underline{k}} - h^{\mathrm{HF,f}}_{\alpha\,\gamma}(t)\right\} g^{\mathrm{f}}_{\gamma\,\beta}(t,t') - \int_C \mathrm{d}\bar{t}\, \Sigma^{\mathrm{f}}_{\alpha\gamma}(t,\bar{t}) g^{\mathrm{f}}_{\gamma\beta}(\bar{t},t') = \delta_{\alpha\beta}\delta_C(t,t')\,.$$

$$\left\{\mathrm{i}\partial_t\delta_{\alpha\beta} - h^{\mathrm{HF,f}}_{\alpha\beta}(t)\right\} G^{\mathrm{fe}}_{\beta\underline{j}}(t,t') - \int_C \mathrm{d}\bar{t}\, \Sigma^{\mathrm{f}}_{\alpha\beta}(t,\bar{t}) G^{\mathrm{fe}}_{\beta\underline{j}}(\bar{t},t') = h^{\mathrm{HF,fe}}_{\alpha\,\underline{k}}(t) G^{\mathrm{e}}_{\underline{k}\underline{j}}(t,t') + \int_C \mathrm{d}\bar{t}\, \Sigma^{\mathrm{fe}}_{\alpha\underline{k}}(t,\bar{t}) G^{\mathrm{e}}_{\underline{k}\underline{j}}(\bar{t},t')$$

[37] M. Bonitz, K. Balzer, H. Ohldag, to be published

Three-layer NEGF embedding scheme: final equations[39] $f \to e \to s$

$$\left\{\mathrm{i}\partial_t \delta_{ik} - h^{\mathrm{HF,s}}_{ik}(t)\right\} G^{\mathrm{s}}_{kj}(t,t') = \delta_{ij}\delta_C(t,t') + \int_C \mathrm{d}\bar{t}\, \tilde{\Sigma}^{\mathrm{s}}_{ik}(t,\bar{t}) G^{\mathrm{s}}_{kj}(\bar{t},t')\,, \qquad \tilde{\Sigma}^{\mathrm{s}} := \Sigma^{\mathrm{s}} + \Sigma^{\mathrm{emb,s}}$$

$$\Sigma^{\mathrm{emb,s}}_{ik}(t,\tilde{t}) = \int_C \mathrm{d}\bar{t} \int_C \mathrm{d}\bar{\bar{t}} \left[h^{\mathrm{HF,se}}_{i\,\underline{k}}(\bar{t})\,\delta_C(t,\bar{t}) + \Sigma^{\mathrm{se}}_{i\,\underline{k}}(t,\bar{t})\right] g^{\mathrm{e}}_{\underline{i}\,\underline{i}}(\bar{t},\bar{\bar{t}}) \left\{h^{\mathrm{HF,es}}_{\underline{i}\,k}(\bar{\bar{t}})\,\delta_C(\bar{\bar{t}},\tilde{t}) + \Sigma^{\mathrm{es}}_{\underline{i}\,k}(\bar{\bar{t}},\tilde{t})\right\},$$

$$\left\{\mathrm{i}\partial_t \delta_{\underline{i}\,\underline{k}} - h^{\mathrm{HF,e}}_{\underline{i}\,\underline{k}}(t)\right\} g^{\mathrm{e}}_{\underline{k}\,\underline{j}}(t,t') = \delta_{\underline{i}\,\underline{j}}\delta_C(t,t') + \int_C \mathrm{d}\bar{t}\, \tilde{\Sigma}^{\mathrm{e}}_{\underline{i}\underline{k}}(t,\bar{t}) g^{\mathrm{e}}_{\underline{k}\underline{j}}(\bar{t},t')\,, \qquad \tilde{\Sigma}^{\mathrm{e}} := \Sigma^{\mathrm{e}} + \Sigma^{\mathrm{emb,e}}$$

$$\Sigma^{\mathrm{emb,e}}_{\underline{i}\underline{j}}(t,\tilde{t}) = \int_C \mathrm{d}\bar{t} \int_C \mathrm{d}\bar{\bar{t}} \left[h^{\mathrm{HF,ef}}_{\underline{i}\,\gamma}(\bar{t})\,\delta_C(t,\bar{t}) + \Sigma^{\mathrm{ef}}_{\underline{i}\,\gamma}(t,\bar{t})\right] g^{\mathrm{f}}_{\gamma\delta}(\bar{t},\bar{\bar{t}}) \left\{h^{\mathrm{HF,fe}}_{\delta\,\underline{j}}(\bar{\bar{t}})\,\delta_C(\bar{\bar{t}},\tilde{t}) + \Sigma^{\mathrm{fe}}_{\delta\,\underline{j}}(\bar{\bar{t}},\tilde{t})\right\},$$

$$\left\{\mathrm{i}\partial_t \delta_{\alpha\gamma} - h^{\mathrm{HF,f}}_{\alpha\gamma}(t)\right\} g^{\mathrm{f}}_{\gamma\beta}(t,t') - \int_C \mathrm{d}\bar{t}\, \Sigma^{\mathrm{f}}_{\alpha\gamma}(t,\bar{t}) g^{\mathrm{f}}_{\gamma\beta}(\bar{t},t') = \delta_{\alpha\beta}\delta_C(t,t')\,.$$

- Closed equation for G^s for arbitrary (e.g. hierarchical) environment. Consistent. Conserving
- Advantage: use increasingly simpler selfenergies and optimized basis sets for s, e, f.[38]
- For non-local selfenergies 2-time computation of g^e scales as N_t^5, and of G^s as N_t^{10}
- G1–G2 scheme remains at N_t^1, but contains increased set of equations ($G^{\alpha\beta}$, $\mathcal{G}^{\alpha\beta\gamma\delta}$)

[38] Analogous to TD-RASCI, D. Hochstuhl, C. Hinz, and M. Bonitz, EPJ-Special Topics **223**, 177-336 (2014)
[39] M. Bonitz, K. Balzer, H. Ohldag, to be published